J. Fluid Mech. (1990), *vol.* 212, *pp.* 209–240
Printed in Great Britain

The fluid mechanics of solidification

By HERBERT E. HUPPERT

Institute of Theoretical Geophysics *and* Department of Applied Mathematics and Theoretical Physics, University of Cambridge, Silver Street, Cambridge CB3 9EW, UK

(Received 22 June 1989)

Intense fluid motions can be generated by the solidification of a binary liquid. This review paper describes systematically some of the concepts involved in the fluid mechanics of solidification. It also presents quantitative calculations for the fluid motion, the rate of growth of solid and the evolution of both the thermal and the compositional fields in various geometries. The results of many of the calculations are favourably compared with data from laboratory experiments using aqueous solutions.

1. Introduction

The subject of fluid mechanics is taught to students and studied by some of the staff in almost all departments of applied mathematics and engineering. In addition, aspects of the subject that can be related to the currently fashionable area of chaos have generated considerable excitement in many departments of physics (Gleick 1988). The subject of solid mechanics is also taught and studied in many of the same departments. The relative strengths in the two areas varies of course from department to department and in an interesting way from country to country. The transition from fluid to solid, however, is far less frequently addressed. Such transitions are very important to metallurgists who consider how melts solidify in complicated shaped moulds to form solid products. Geologists are trained to evaluate the conditions of temperature, concentration and pressure under which a silicate melt will solidify at thermodynamic equilibrium, but the fluid-mechanical processes which interact with solidification have, by and large, been incorporated into geological models only recently. A good course in physics includes a discussion of the atomic rearrangement accompanying solidification but macroscopic analyses and the resulting fluid dynamical effects are rarely included.

The aim of this paper is to review some of the recent work on the fluid-mechanical phenomena that accompany and can play an important role in solidification. In particular, it will discuss a new slant on the general approach of continuum mechanics that needs to be introduced to analyse the formation of *mushy zones* and *slurries*; regions in which fluid and solid coexist. The topic suggests many new research problems from both a theoretical and an experimental point of view which may be found attractive to applied mathematicians, engineers and fluid dynamicists as well as being of fundamental importance to at least crystal growers, geologists and metallurgists.

Fluid mechanics can play a fundamental role in the phase transitions that accompany solidification because when a liquid of two or more components solidifies, the composition of the solid product generally differs from that of the original liquid. For example, salty water in the polar oceans freezes to form almost pure ice, while

in the semi-conductor industry melts containing comparable quantities of gallium and germanium could be partially solidified to form almost pure germanium. The difference in composition between liquid and solid implies that the composition of the liquid in the neighbourhood of the solidification front can be different from that further away. This difference in composition is generally associated with a difference in density, which can drive fluid motions, transport both heat and mass convectively and alter the rate and maybe even the mode of the solidification processes.

There are a number of different approaches that have been used to investigate solidification phenomena. One is to consider the growth of individual crystals following the famous similarity solution determined originally by Ivantsov (1947) for the steady growth from a one-component melt of a single crystal modelled as a paraboloid of revolution. This shape was found theoretically to be unstable to secondary and tertiary side branches (Langer 1980) which are a common feature in some crystals, in particular snow flakes. (An interesting survey appears in chapters 3 and 4 of Kurz & Fisher 1986.) The most recent developments on systems free of surface energy are lucidly described by Canright & Davis (1989), who investigate the similarity solution for the growth from a multi-component melt of a single crystal with the interface between fluid and solid modelled as a general quadric surface. Their study also includes the effects of both a nonlinear phase diagram at thermodynamic equilibrium and cross-diffusion due to either the Soret or Dufour effects. Some fluid mechanics has been included in the investigation by the incorporation of a flow at low Reynolds number past the crystal, but neglecting any effects due to gravity (Ananth & Gill 1988, 1989 and Canright & Davis 1989). In addition, an extremely elegant series of experiments on doubly purified succinonitrile has been conducted by Glicksman and his colleagues and led to the photographs reproduced as figure 1 in Glicksman, Coriell & McFadden (1986). The experiments demonstrated that gravity can play a dominant role, at least in determining the shape of a single crystal. However, no theoretical investigation has to my knowledge been undertaken of the coupling between solidification and the fluid mechanics of convection driven by the growth of a single crystal in a gravitational field. Furthermore, it is not at all clear how to use the results for the growth of a single crystal to predict effects arising from the macroscopic growth of a field of crystals.

Another approach is to employ numerical simulations. This will be particularly important for assessing the effects of solidification in complex industrial moulds. Some concepts have been elucidated by this approach and are comprehensively reviewed by Brown (1988). However, many numerical schemes neglect any fluid motions and it is sometimes difficult to find the fundamental principles hidden in the vast quantity of numerical output.

A third approach, parts of which I intend to review here, is to consider a series of situations which sequentially bring out the main concepts involved in the fluid mechanics of solidification. The review inevitably emphasizes the contributions I have made, often in collaboration with my colleagues both in Cambridge and at the Australian National University. Reviews written with different emphases include Langer (1980), Coriell, McFadden & Sekerka (1985), Glicksman *et al.* (1986), Langer (1987), some of the papers published and listed in the bibliography in Loper (1987) and Davis (1990).

My own investigations in this field commenced with the consideration of the principles involved in the fundamental situation of cooling an initially homogeneous two-component melt at a single horizontal boundary (Huppert & Worster 1985). We identified six different flow regimes dependent upon whether the cooling takes place

at an upper or lower boundary to the melt and whether the density of the fluid released on solidification is the same, greater or less than that of the melt. This differentiation between the flow regimes is one of the major concepts upon which the review is based.

In the next section we consider the cooling from below of a liquid which is compositionally identical to its solidified product. We identify the situation as a classical Stefan problem, a problem which has no fluid-mechanical ingredient. In §3 we consider the influence of the unstable thermal field that results from cooling such a fluid from above. Section 4 incorporates effects due to compositional differences for the first time by considering the cooling and crystallizing from below of a liquid that releases fluid of greater density when solidifying. We indicate that the moving interface between fluid and solid is generally unstable, which leads to the formation of a mushy layer. We describe a simple theoretical model for this mushy layer and demonstrate that predictions of the model agree well with data from our laboratory experiments.

In §5 we extend the theoretical model in a study of the solidification by cooling from above a liquid which also releases less dense fluid. Assuming first that solidification occurs at thermodynamic equilibrium and that the cooling temperature exceeds the eutectic temperature, we determine the rate of growth of the mushy layer that forms on the roof. The agreement between the theoretical predictions and the laboratory data is good, but not perfect. The agreement is improved on the incorporation of non-equilibrium effects into the model by specifying a relationship between the rate of growth of the mushy layer and the non-equilibrium undercooling at the interface between mush and liquid.

Effects due to lowering the cooling temperature below the eutectic temperature are discussed in §6. We describe how this can lead to compositional stratification in the solid. In addition, we explain how cooling at the top of a container can lead to solidification at the base – a result relevant to the cooling of a large magma chamber, or storage chamber of liquid rock, from above. The special effects observed when cooling aqueous ammonium chloride are briefly described in §7. Global two-dimensional effects, which result from cooling at either a vertical or a sloping wall, are discussed in §§8 and 9. A very brief description of some of the applications of our general concepts makes up §10 which is followed by a short concluding section.

Any study of solidification must be based on the phase diagram, which specifies the possible states of liquid and solid at thermodynamic equilibrium as a function of temperature and composition (and possibly also pressure). Readers who are unacquainted with the concepts of phase diagrams may care to read Kurz & Fisher (1986) along with the brief description that follows. A typical phase diagram for a two-component system, made up of components A and B, is sketched in figure 1. Above the liquidus, which has two branches, the system is totally liquid. If the temperature falls below the liquidus, a solid whose composition is given by the appropriate branch of the solidus is formed. Liquids with initial compositions between A and C_E first crystallize a and follow the liquidus curve as they cool. The remaining liquid is residually enriched in component B and its bulk density increases. When the liquid composition reaches the eutectic at E, b begins to crystallize and the two phases a and b continue to solidify at the fixed temperature T_E until all the liquid is consumed. A liquid with initial composition between C_E and B would follow a similar course but crystallizes b first rather than a and the residual liquid decreases in bulk density. Thus above the eutectic temperature T_E (and still below the liquidus curve), liquid and solid phases can coexist. For temperatures below the eutectic line,

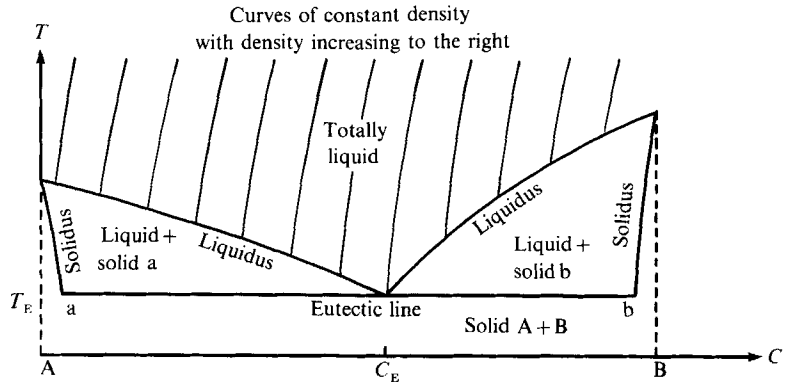

FIGURE 1. A typical phase diagram for a binary mixture, made up of components A and B, which indicates the phases at thermodynamic equilibrium as functions of temperature, T, and concentration of component B, which is denoted by C. The dashed vertical lines at constant concentration represent the solidii for most aqueous solutions.

only solid phases can form, at least under the constraint of thermodynamic equilibrium. For almost all aqueous solutions the solidii are vertical which means that the composition of the solid formed is independent of temperature (and thus a and A coincide as do b and B).

Density in the liquid is generally a very much stronger function of composition than of temperature, as is sketched in figure 1. This is the explanation of why a melt whose composition is less than the eutectic composition C_E releases more dense fluid, while a melt whose composition exceeds C_E releases less dense fluid when the fluid is cooled and solidified.

2. The classical Stefan problem

One of the simplest situations in which a melt undergoes a phase change and is transformed into a solid is as follows. The semi-infinite region $z > 0$ consists of material which is initially liquid and at uniform temperature T_∞. At $t = 0$ the temperature at the base of the fluid at $z = 0$ is suddenly lowered to T_B and subsequently maintained at that value, which is less than the solidification temperature of the melt, T_s, as depicted in figure 2. The problem is to determine the position of the unknown, moving solidifying interface, $s(t)$, and the temperature distributions, $T(z, t)$, in both the liquid and the solid phase in this one-dimensional problem.

Our analysis commences with the assumption that there is no motion in the melt and that compositional effects play no role in the solidification. This requires the constituents of the melt and the solid to be identical. Generally this means a one-component, or pure, melt, such as water or liquid gold for example; with respect to the phase diagram that makes up figure 1 we are considering the composition to be either pure A or pure B. However, binary melts of eutectic composition C_E also produce solids that have the same composition as the original liquid. Throughout the discussion we shall neglect any difference in density between solid and liquid, which is generally a small effect. The requirement of no motion then means that the thermal field must be stably distributed, which for those melts whose density increases with temperature indicates that the z-axis is directed vertically upwards.

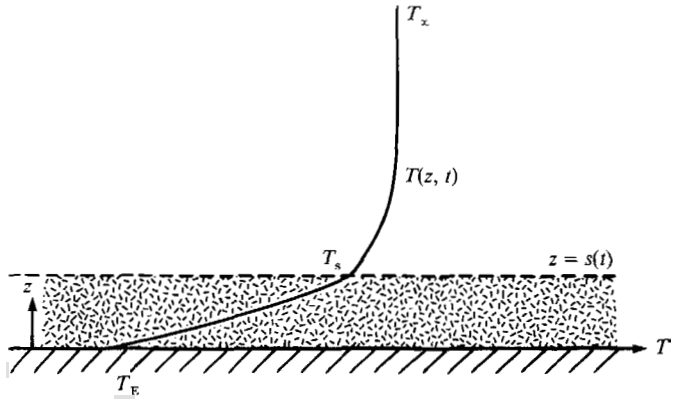

FIGURE 2. Sketch of the temperature profile and notation for a semi-infinite one-component melt cooled from below.

Mathematically, the problem requires the solution of the heat-conduction equations

$$T_t = \kappa_s T_{zz} \quad (0 < z \leqslant s(t)) \tag{2.1a}$$

and

$$T_t = \kappa_m T_{zz} \quad (s(t) \leqslant z), \tag{2.1b}$$

where κ is the thermal diffusivity, with subscripts s and m denoting values in the solid and melt, respectively. The regions occupied by the two phases are linked by the conservation of heat flux at the interface, which can be written

$$\mathscr{L}\dot{s} = k_s T_z|_{s-} - k_m T_z|_{s+}, \tag{2.2}$$

where $\mathscr{L}$ is the latent heat per unit volume of solid and k is the thermal conductivity. Finally, there are the boundary conditions on the temperature

$$T = T_B \quad (z = 0), \qquad T \to T_\infty \quad (z \to \infty \text{ or } t \to 0). \tag{2.3a, b}$$

Because there is no externally imposed lengthscale in the problem, a similarity solution must exist of the form

$$s(t) = 2\lambda_2(\kappa_s t)^{\frac{1}{2}}, \tag{2.4}$$

with λ_2 satisfying an eigenvalue relationship of the form

$$F\left(\lambda_2; \mathscr{S}, \frac{T_\infty - T_s}{T_s - T_B}, \frac{k_s}{k_m}, \frac{\kappa_s}{\kappa_m}\right) = 0 \tag{2.5}$$

(Carslaw & Jaeger 1959, §11.2), where the Stefan number

$$\mathscr{S} = \frac{\mathscr{L}}{c_s(T_s - T_B)} \tag{2.6}$$

and c_s is the specific heat per unit volume of the solid. The Stefan number represents the ratio of two quantities: the latent heat needed to transform the melt into solid and the heat needed to cool the solid from its solidification temperature to the temperature at the boundary.

The solution (2.5) appears to have been first presented by Lamé & Clapeyron (1831). It was then discussed in a famous series of (unpublished) lectures given by

Neumann in Königsberg in the early 1860's and reappeared in Stefan (1889). It is the solution of the simplest of a huge variety of moving boundary problems involving melting or solidification generally known as 'Stefan problems'. Admirable discussions of Stefan problems are contained in Crank (1984), Hill (1987) and references therein. Very few exact analytical solutions exist and the area has been a haven for applied mathematicians who have developed a variety of approximate and/or numerical techniques to obtain solutions.

But, of course, no fluid *dynamics* is involved; indeed hardly even fluid *statics*.

3. Cooling a pure melt from above

Fluid mechanics becomes involved if the situation considered in figure 2 is inverted to form figure 3(*a*) and the pure melt is considered to be cooled from above. The resulting temperature in the melt increases with depth and thus a fluid instability is possible. A combined experimental and theoretical investigation of the conditions for which instability is initiated and the form of convection in the melt has been carried out by Davis, Müller & Dietsche (1984) and Dietsche & Müller (1985). They held the temperatures T_A and T_B at the lower and upper boundaries fixed and determined, from the solution of a steady-state problem, the critical value of the Rayleigh number

$$Ra = \alpha g(T_A - T_s)(H-s)^3/\kappa_m \nu \tag{3.1}$$

for the onset of convection as a function of the ratio, say $\mathscr{A}$, of the depths of solid and liquid in static equilibrium, with

$$\mathscr{A} = \frac{s}{H-s} = \left(\frac{k_s}{k_m}\right)\left(\frac{T_s - T_B}{T_A - T_s}\right), \tag{3.2a, b}$$

where α is the coefficient of expansion, g the acceleration due to gravity and H the total depth of the system. They then employed weakly nonlinear perturbation theory to predict the form of the convective motions – rolls, hexagons or mixed polygonal rolls – for Rayleigh numbers just above critical. These theoretical predictions were in good qualitative agreement with their experiments using cyclohexane, which showed picturesque deformations at the interface between solid and melt due to convection coupled to the melting and freezing.

Numerous theoretical studies of directional solidification have been undertaken using the techniques of weakly nonlinear perturbation theory (see, for example, Coriell *et al.* 1985). There has been some agreement between the theoretical results of these studies and experimental observations, but generally, in natural, industrial and even most experimental situations, the conditions are well away from those for which weakly nonlinear theory is applicable.

When, for example, in the geometry considered by Davis *et al.* (1984), the Rayleigh number is very much larger than the critical value and sufficiently high that the convection in the melt is turbulent, a different parameterization to the one they considered is appropriate. Turner, Huppert & Sparks (1986, herein referred to as THS) examined the situation depicted in figure 3(*b*) where the lower boundary is insulated, rather than being maintained at a fixed temperature. This allows the temperature to evolve with time and leads eventually to total solidification. The relevant conduction equation in $0 < z \leqslant s(t)$ is again given by (2.1*a*). In the melt the

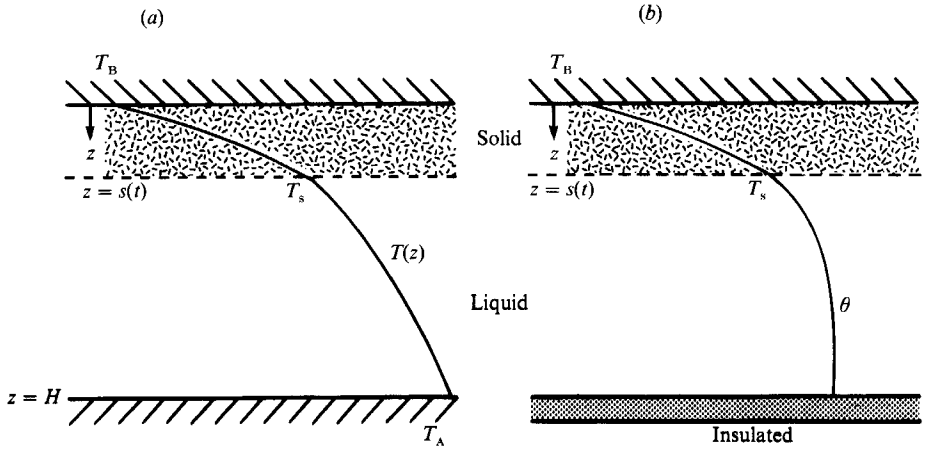

FIGURE 3. Sketch of the temperature profile and notation for a one-component melt of initial depth H cooled from above. Note that in (a) the lower boundary is at a fixed temperature while in (b) the lower boundary is insulated.

heat transfer can be described by the well-known four-thirds law (Turner 1979) so that

$$-c_m(H-s)\,\dot{\theta} = F_T = \gamma k_m \left(\frac{\alpha g}{\kappa_m \nu}\right)^{\frac{1}{3}} (\theta - T_s)^{\frac{4}{3}}, \tag{3.3a, b}$$

where θ is the mean temperature of the melt, F_T is the thermal flux at the interface and γ is an empirical constant. The interfacial condition (cf. (2.2)) is

$$k_s T_z|_{s-} = F_T + [c_m(\theta - T_s) + \mathscr{L}]\dot{s}. \tag{3.4}$$

This equation represents a balance of the conductive transfer through the solid with the convective transfer in the melt in addition to the heat released by decreasing the temperature of the melt to the solidification temperature and then solidifying it. Each of these terms is always positive and so in particular the term on the left-hand side always contributes in an essential way to the heat balance. Either of the other two terms may also dominate the heat balance and this leads to three different regimes. Within each regime conduction balances either convection, latent heat release or both, as discussed at length by THS. They present both asymptotic and numerical solutions to the equations as well as data from a variety of experiments which, as far as they go, support the theoretical predictions. It might be interesting to carry out further experiments in parameter ranges different from those treated experimentally by THS yet falling within the range of their theory.

4. Cooling a binary alloy from below

Some of the fluid-mechanical effects due to compositional differences between melt and solid can now be easily introduced by investigating the solidification that results from cooling a binary alloy from below. We first consider the situation in which the fluid released by the solidification process is relatively dense and so ponds above the solid. We shall assume the solid to be of fixed composition (a vertical solidus) as will result, for example, if ice is formed from the cooling of an aqueous solution. We also assume, at least initially, that the interface at $z = s(t)$ between solid and melt is flat

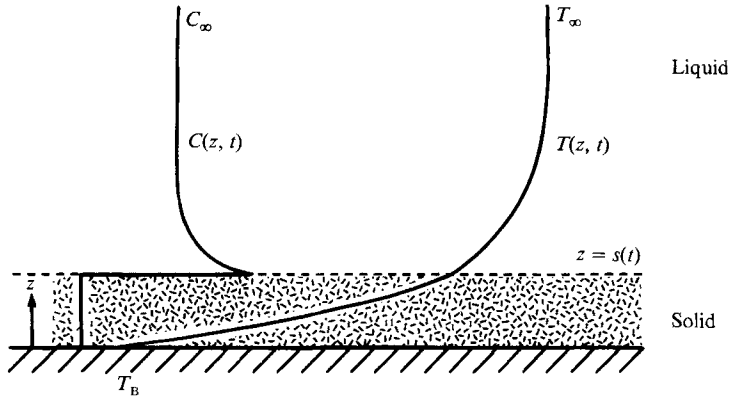

FIGURE 4. Sketch of the stably distributed temperature and composition profiles for a semi-infinite binary melt cooled from below to form a stable one-dimensional interface between melt and solid on the release of melt whose density exceeds that of the original melt.

(and horizontal) so that the problem is totally one-dimensional. No motion will occur in the melt and the transport of both heat and chemical components is entirely by molecular diffusion. This leads to profiles of both temperature and composition which are stably distributed, as is sketched in figure 4.

The equations governing the temperature profiles are exactly as in §2: the heat-conduction equation (2.1), the thermal conservation condition (2.2) and the thermal boundary condition (2.3). The compositional profile relative to that in the solid $C(z,t)$ is governed in the melt by

$$C_t = DC_{zz} \quad (s(t) \leqslant z), \tag{4.1}$$

where D is the coefficient of compositional diffusivity, while the composition in the solid will be expressed as $C = 0$. Conservation of solute requires that

$$C\dot{s} + DC_z = 0 \quad (z = s(t)+) \tag{4.2}$$

and the initial, or far-field, condition on the composition, to complement that on the temperature (2.3b), is

$$C \to C_\infty \quad (z \to \infty \text{ or } t \to 0). \tag{4.3}$$

As briefly discussed in the introduction, in a binary liquid that solidifies at thermodynamic equilibrium, the temperature of solidification T_s and the composition of the melt at the interface are connected by the liquidus relationship. In many situations a linear relationship of the form

$$T = -m_L C, \tag{4.4}$$

where m_L is a positive constant, is an adequate approximation. Note that the form of (4.4) assumes the liquidus temperature is zero at zero concentration.

The mathematical system (2.1)–(2.3), (4.1)–(4.3) and (4.4) applied at $z = s(t)$ admits a similarity solution of the form

$$s = 2\lambda_4 (Dt)^{\frac{1}{2}}, \tag{4.5}$$

with λ_4 satisfying an eigenvalue relationship of the form

$$F\left(\lambda_4; \mathscr{P}, \frac{T_\infty - T_L}{T_L - T_B}, \frac{T_L}{T_B}, \frac{k_s}{k_m}, \frac{\kappa_s}{\kappa_m}, \frac{D}{\kappa_m}\right) = 0 \tag{4.6}$$

(Rubenstein 1971; Worster 1983; Huppert & Worster 1985), where the modified Stefan number

$$\tilde{\mathscr{S}} = \frac{\mathscr{L}}{c_s(T_L - T_B)} \tag{4.7}$$

and $T_L = -m_L C_\infty$ is the liquidus temperature at the initial concentration. The resulting temperature and composition fields are drawn in figure 4.

Huppert & Worster (1985) carried out a series of experiments in which aqueous solutions of $NaNO_3$, NaCl and NH_4Cl were cooled in the apparatus sketched in figure 5. In each experiment, after a short initial period the thickness of the solid block (ice) increased with the square root of time, as predicted by (4.5). Four typical results for the measured growth-rate eigenvalue λ_4 at different initial compositions C_∞ are plotted in figure 6 and compared with the theoretical relationship (4.6). The agreement is abysmal. Why?

The reason for the disagreement is that under almost all conditions the solid, in this case ice, does not grow with a stable planar interface. During solidification, solute is removed from the melt and a diffusion profile develops in that part of the melt that is adjacent to the interface between melt and solid. In the one-dimensional growth sketched in figure 4 the relatively slow compositional diffusion, which is governed by the value of $D(\ll \kappa_m$ or $\kappa_s)$, constrains the rate of growth of the interface. Instead, the interface in the experiments becomes highly irregular, as seen in the photographs of ice reproduced in figure 7 (plate 1). The initial breakup of a planar interface is known as morphological instability and was considered at a qualitative level by Rutter & Chalmers (1953). They suggested that instability occurred whenever

$$-m_L C_z > T_z (> 0) \quad (z = s(t)+) \tag{4.8}$$

because the temperature and composition fields predicted by the one-dimensional model on the melt side of the interface would then be below the liquidus, which implies (inconsistently) that the melt is in the solid field. Quantitative dynamical calculations (but neglecting convective motions in the melt) were undertaken some years later by Mullins & Sekerka (1964) to lead to the instability criterion

$$-(k_s + k_m) m_L C_z|_{s+} > k_s T_z|_{s-} + k_m T_z|_{s+} \tag{4.9}$$

if surface tension effects at the interface are ignored. This criterion reverts formally to (4.8) if k_s is set equal to zero. Because the thermal and compositional field are both stably stratified no convection can take place in the melt. This is in contrast to the case where the solidification releases light fluid, although numerical calculations incorporating the possibility of convection in the melt (Coriell *et al.* 1980 and Hurle, Jakeman & Wheeler 1982) lead to results which under usual conditions differ little from either (4.8) or (4.9). A nice general review of the interaction between solidification and linear convection is presented in Glicksman *et al.* (1986) and a section in Davis (1990) is also devoted to this topic. All calculations indicate that only for very small values of both the undercooling $T_s - T_B$ and resulting interfacial velocity $\dot{s}$ is the interface stable, as is presented quantitatively by Huppert & Worster (1985) in their figure 1. Paradoxically, no experiment has yet been performed that distinguishes between the slightly different predictions embodied in (4.8), (4.9) and the numerical calculations including the effects of linear convection in the melt. This reflects the fact that only for very special conditions will the planar interface be stable.

In order to reconcile theory and experiment, Huppert & Worster (1985) developed

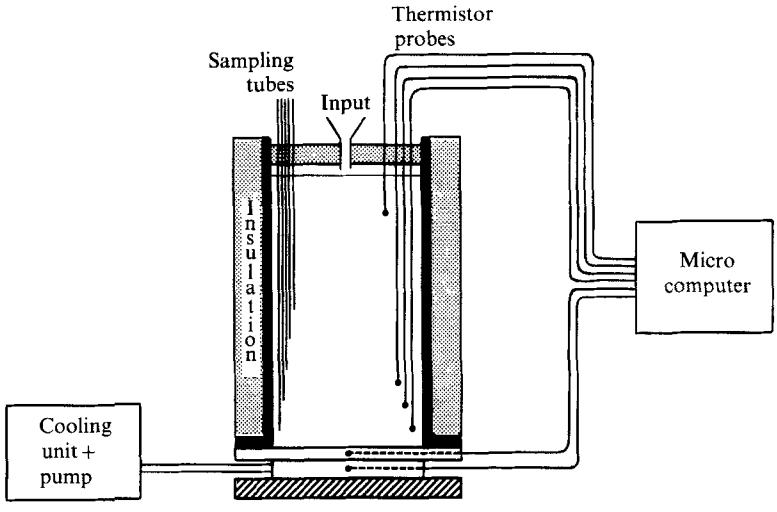

FIGURE 5. Sketch of the apparatus used by Huppert & Worster (1985) to cool and solidify various aqueous solutions.

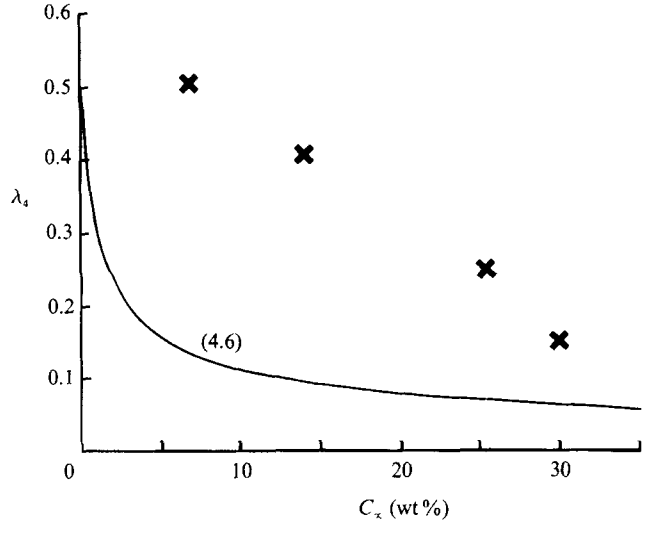

FIGURE 6. The non-dimensional growth rate λ_4 as a function of the initial far-field composition, C_∞, for stable, one-dimensional solidification from below of aqueous $NaNO_3$ with $T_B = -17$ °C and $T_\infty = 15$ °C. The solid curve represents the theoretical relationship (4.6) and the crosses represent experimental data.

a simple model of the solidification which incorporated a mushy layer in which solid and melt coexist, as observed in their experiments. They postulated that the mush could be described by a constant solid fraction, ϕ, and that global conservation equations, consistent with this idea, could be used to describe the transitions in the mushy layer. The resulting thermal and compositional fields are sketched in figure 8. The temperature field satisfies

$$T_t = \bar{\kappa} T_{zz} \quad (0 < z \leqslant s(t)) \tag{4.10a}$$

$$T_t = \kappa_m T_{zz} \quad (s(t) \leqslant z) \tag{4.10b}$$

and

$$\mathscr{L}\phi\dot{s} = \bar{k} T_z|_{s-} - k_m T_z|_{s+}, \tag{4.10c}$$

FIGURE 7. A photograph taken in the vertical plane which reveals the form of the resulting product obtained by cooling an aqueous solution of $NaNO_3$ to form ice. Note the uneven upper surface and the almost vertical crevices in the solid ice which contain compositionally enriched fluid. The horizontal scale beneath CB225 is 2 cm long. Conditions of the experiment: $T_B = -16.5°C$, $T = 14.7°C$, $C = 14$ wt% $NaNO_3$.

FIGURE 14. A photograph taken during an experiment in which an aqueous solution of Na_2SO_4 was cooled from above to form a composite layer next to the roof of the tank, a mushy layer below this and a layer of faceted $Na_2SO_4.10H_20$ crystals at the base. The experimental conditions were: $C_0 = 16$ wt % Na_2SO_4, $T_0 = 30.5°C$, $T_B = -17°C$, and $H = 18.8$ cm.

(*Facing p.* 218)

(a)

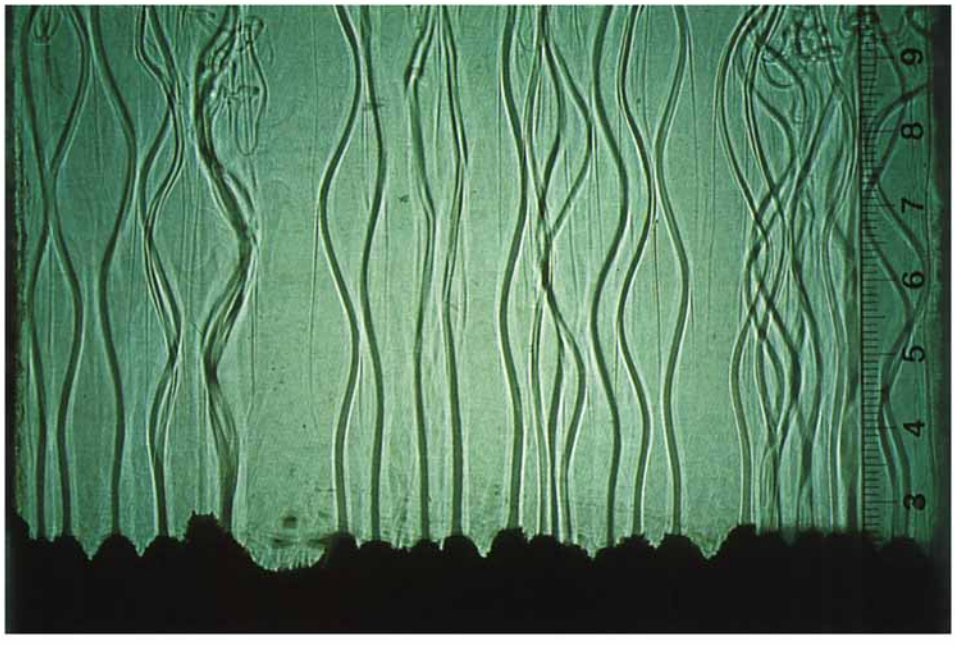

(b)

FIGURE 19. Four views of an experiment in which a 26 wt % solution of aqueous NH_4Cl with a small amount of green dye added is cooled from below. *(a)* A vertical view taken in shadowgraph showing plumes rising from individual vents. *(b)* A vertical view of the NH_4Cl crystals, after draining off all remaining fluid, which shows clear secondary and tertiary branching behind the crystal tips. The photograph represents approximately 8 mm in the horizontal. *(c)* An oblique view of the tops of the chimneys from which plumes rise. *(d)* A horizontal view of an individual vent after all the fluid has been drained off.

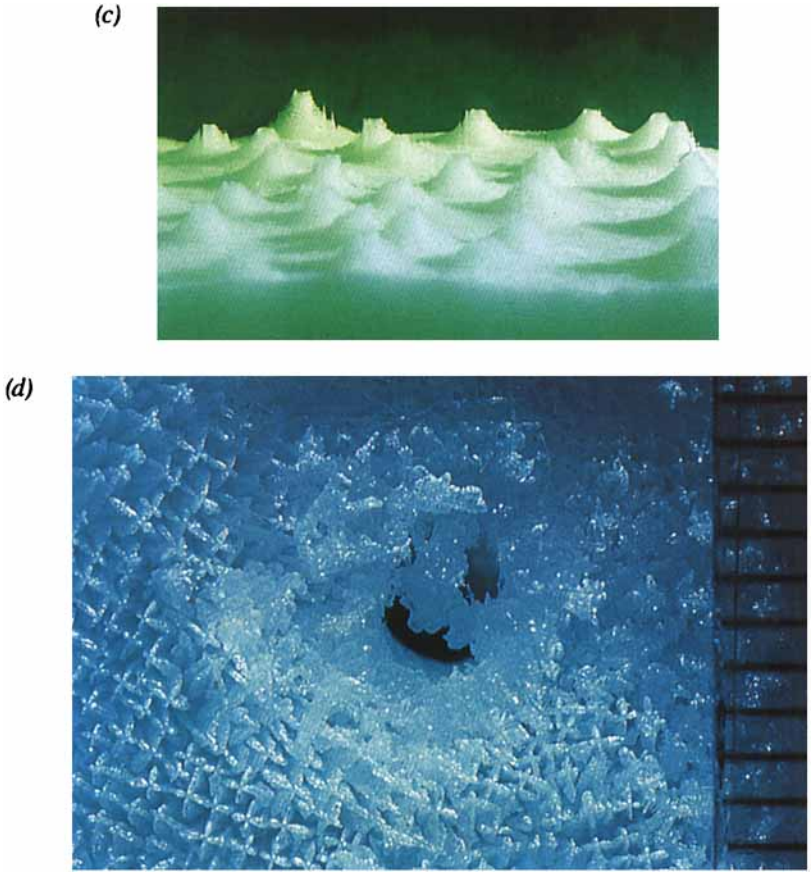

FIGURE 19 *(c, d)*. For caption see Plate 2.

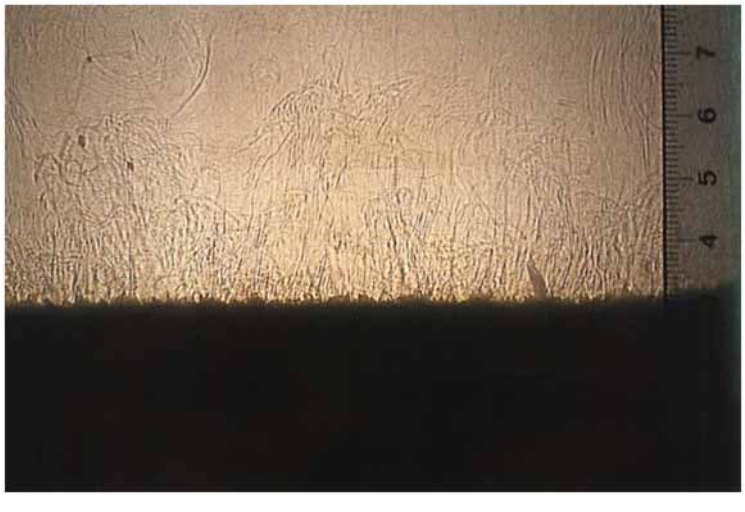

FIGURE 20. A vertical shadowgraph view of a 13 wt % solution of Na_2CO_3 cooled from below with $T_B = -20°C$. Compare the form of the flow field with that of figure 19 *(a)*.

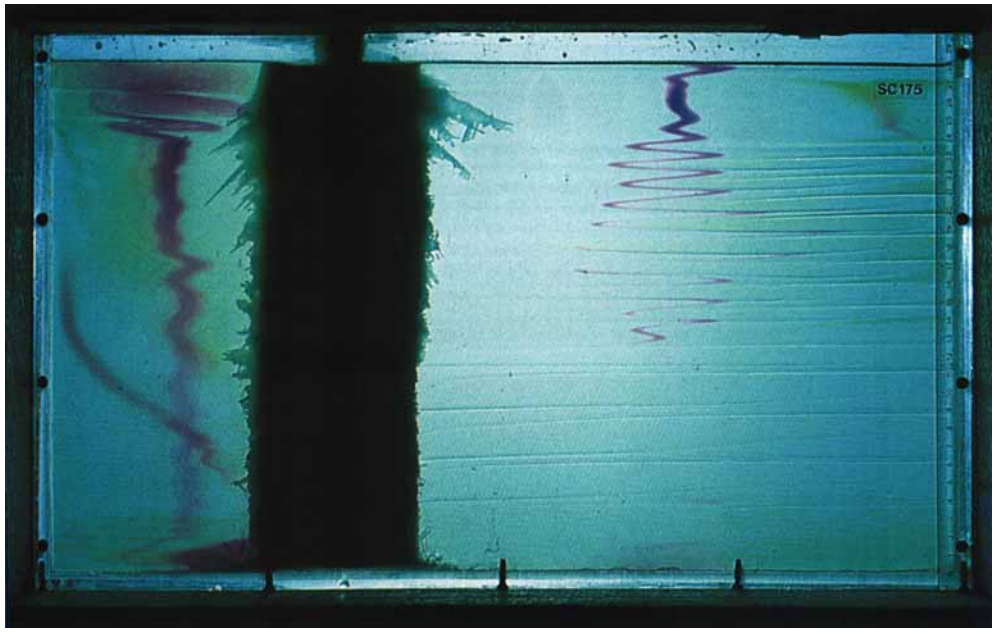

FIGURE 22. A photograph of an experiment cooling two containers of aqueous Na_2CO_3 at a vertical wall. In both containers C_0 = 13 wt %, T_0 = 19°C, T_B = −20°C. The dye trace results from $KMnO_3$ crystals inserted into the liquid 3 min before the photograph was taken.

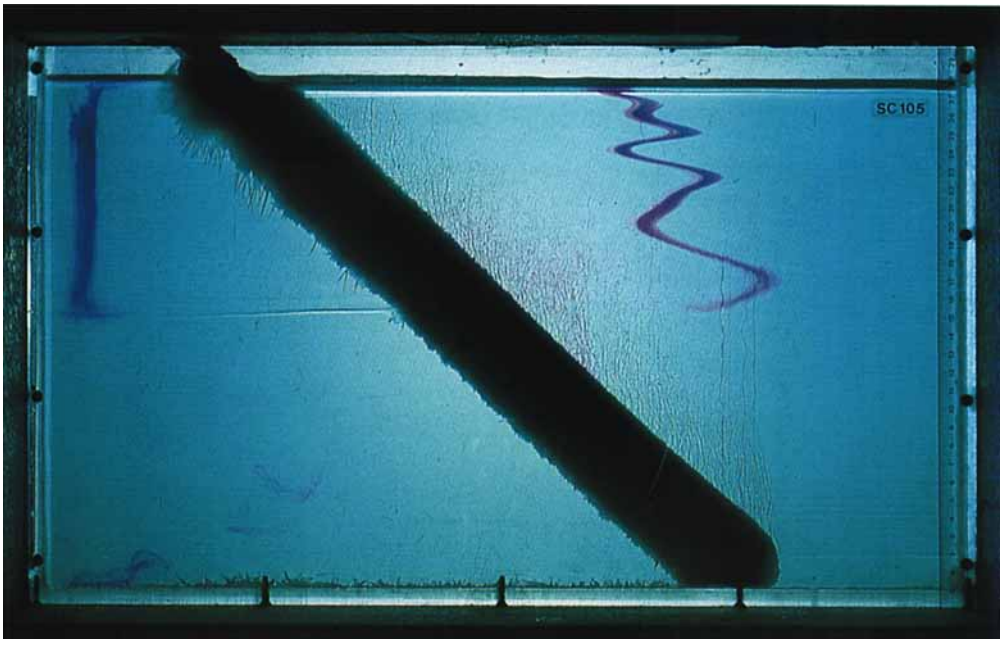

FIGURE 25. A photograph of an experiment cooling an aqueous solution of Na_2CO_3 at a 45° slope with C_0 = 13 wt %, T_0 = 19°C, T_B = −20°C. The dye trace results from $KMnO_3$ crystals inserted into the liquid 4 min before the photograph was taken.

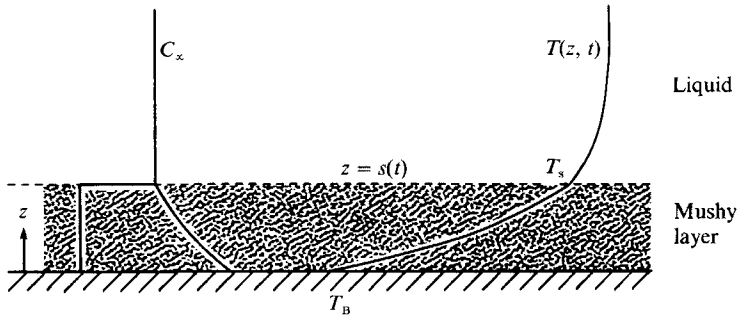

FIGURE 8. Sketch of the temperature and composition profiles for a semi-infinite binary melt cooled from below to form a mushy layer on the release of liquid whose density exceeds that of the original melt.

where an overbar denotes values in the mush. These quantities are evaluated using averages weighted by the volume fraction to obtain

$$\bar{k} = \phi k_s + (1-\phi)\, k_m = \bar{c}\bar{\kappa}, \tag{4.11a, b}$$

where

$$\bar{c} = \phi c_s + (1-\phi)\, c_m. \tag{4.11c}$$

The representation (4.11*a*) is a good approximation for a random mixture of solid and liquid and becomes exact if the solid dendrites are of constant width and grow vertically (Batchelor 1974). The expression (4.11*c*) is always correct. In the mushy layer the composition is either zero in the solid dendrites or at the local liquidus in the interstitial melt; that is

$$C = -T/m_L \quad (0 < z \leqslant s(t) \text{ within the interstitial melt}). \tag{4.12}$$

The composition field in the melt is negligibly influenced by the rapid growth of the mushy layer because of the small value of the compositional diffusivity, and so

$$C = C_\infty \quad (s(t) \leqslant z). \tag{4.13}$$

Global conservation of solute requires that

$$(1-\phi)\int_0^{s(t)} C(z,t)\,\mathrm{d}z = s(t)\, C_\infty. \tag{4.14}$$

In the model, conservation of solute is achieved by increasing the concentration of the melt within the interstices rather than pushing solute ahead of the advancing solidification front. The growth of solid is thus not constrained by the relatively slow molecular diffusion of composition.

The system comprising (4.10)–(4.14), the boundary and initial conditions on the temperature field (2.3) and the liquidus relationship (4.4) applied at the tips of the dendrites (at $z = s(t)$) has solution

$$s = 2\bar{\lambda}_4(\kappa_m t)^{\frac{1}{2}}, \tag{4.15}$$

where $\bar{\lambda}_4$ satisfies an equation of the form

$$F\left(\bar{\lambda}_4; \mathscr{P}, \frac{c_m(T_\infty - T_L}{\bar{c}(T_L - T_B)}, \frac{\bar{\kappa}}{\kappa_m}\right) = 0, \tag{4.16a}$$

with

$$G\left(\phi; \frac{T_L}{T_B}, \frac{\bar{\kappa}}{\kappa_m}\right) = 0 \tag{4.16b}$$

while
$$\bar{\mathscr{S}} = \frac{\phi \mathscr{L}}{\bar{c}(T_{\mathrm{L}} - T_{\mathrm{B}})} \tag{4.17}$$

is the Stefan number across the mushy layer.

The predictions of the growth rate $\bar{\lambda}_4$ obtained by this approach are seen to agree well with the results of our laboratory experiments, as is shown in figure 9 for one particular series of experiments. Also plotted in the figure is the theoretical value for the (constant) solid fraction ϕ. At the time of the work I did not know how to measure the solid fraction to compare with the predictions. It was suggested to me that an acoustical measurement based on the vastly different speeds of sound in solid and liquid might be possible. This technique proved to be impossible, however, owing to acoustical absorption and scattering in the complex medium. Over the summer of 1989 T. G. L. Shirtcliffe, during a research visit to Cambridge, developed and tested a technique based on differences in electrical conductivity. We plan to write a paper presenting the results in the near future.

The good agreement between the experimental results and the predictions of a model in which the solid fraction was assumed constant throughout was somewhat surprising. Indeed a referee of Huppert & Worster (1985) wrote in his report: 'The explanation of this fact will be challenging to readers (including myself if I could find the time!)'. The challenge was taken up by Worster (1986). He allowed the solid fraction to change in both space and time. Within the mushy layer the local conservation of heat and composition was written as

$$\bar{c}T_t = (\bar{k}T_z)_z + \mathscr{L}\phi_t \tag{4.18}$$

and
$$(1-\phi)\,C_t = (D(1-\phi)\,C_z)_z + C\phi_t, \tag{4.19}$$

where the last term in each of (4.18) and (4.19) represents the release of latent heat into the mush and the release of solute into the interstitial fluid respectively. The introduction of a first-order spatial derivative of ϕ into the mathematical model indicates that an additional boundary condition is required. Worster (1986) argued that the appropriate condition is that of equilibrium saturation, or marginal equilibrium, in the melt just ahead of the growing dendrites, which is expressed as

$$T_z = -m_{\mathrm{L}} C_z \quad (z = s(t)+). \tag{4.20}$$

He showed further that (4.20) under most circumstances is equivalent to the condition

$$\phi = 0 \quad (z = s(t)). \tag{4.21}$$

From the complete system of equations Worster found that there was a similarity solution for which the top of the mush was specified by

$$s = 2\bar{\lambda}_{\mathrm{W}}(Dt)^{\frac{1}{2}}. \tag{4.22}$$

Figure 10 graphs the result for one particular set of parametric values and allows a comparison to be made both with $\bar{\lambda}_4$, obtained by the simpler method outlined above, and with the experimental data. The agreement with both is seen to be very good. Indeed, the full model, though intellectually more satisfying, does not seem to fit these particular observations significantly better than results from the simpler model.

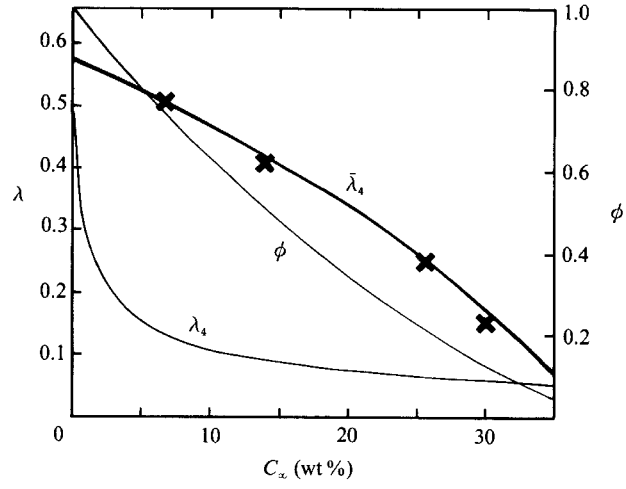

FIGURE 9. The non-dimensional growth rates λ_4 and $\bar{\lambda}_4$ (determined from (4.16)) and the constant solid fraction ϕ for solidification from below with parameters as in figure 6.

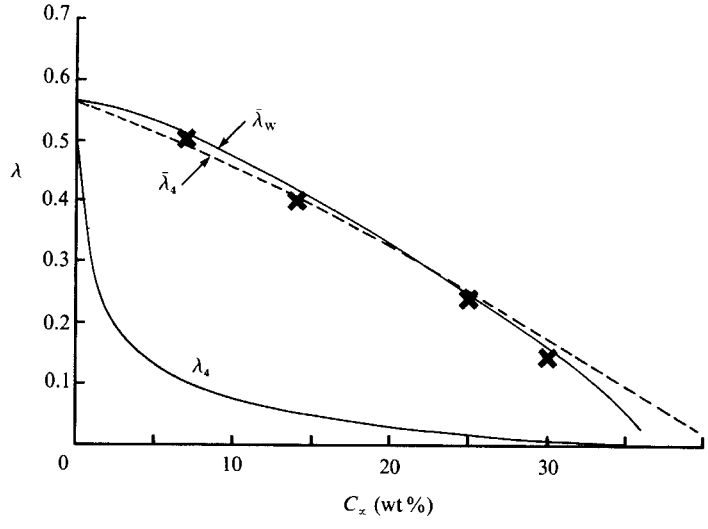

FIGURE 10. The non-dimensional growth rates λ_4, $\bar{\lambda}_4$ and $\bar{\lambda}_w$ (determined by Worster 1986) with parameters as in figure 6.

5. Cooling a binary alloy from above

Additional fluid-mechanical effects occur if a two-component fluid that releases less dense fluid upon solidification is cooled from above. Some of these were identified and catalogued in THS, a study which is greatly extended in a series of recent papers by Kerr *et al.* (1989, 1990*a–c*). In these papers we developed theoretical models to describe new observations and we were able to compare the quantitative predictions of our analysis successfully against the results of our laboratory experiments with aqueous solutions of isopropanol and sodium sulphate. Kerr *et al.* (1989) presents a summary of the detailed analysis and experimental techniques described in Kerr *et al.* (1990*a–c*). In turn, this section highlights the new and important contributions

described in Kerr *et al.* (1989) bearing in mind that a reader interested in any of the details can refer to Kerr *et al.* (1990*a–c*) (after noting that some of the notation is different).

Consider first that T_B, the temperature of the roof at $z = 0$, is less than the liquidus temperature $T_L(C_0)$, where C_0 is the initial composition of the melt, and greater than the eutectic temperature T_E. Our experiments with aqueous isopropanol (with C_0 around 17 wt% isopropanol) in such circumstances led to the formation of ice and the release of an isopropanol-enriched solution. Both the ice and the released solution were less dense than the original solution. A relatively light mushy ice layer, bathed in stagnant, isopropanol-enriched water, thus formed at the top of the container. This cold layer maintained turbulent thermal convection in the fluid below.

We developed the following model to describe this general situation as sketched in figure 11, with the solid fraction ϕ taken to be a function of both z and t. Within the mush, conservation of heat is expressed by (4.18) and conservation of solute by (4.19) with the first term on the right-hand side neglected (formally, D set to 0) following the argument that since $D \ll \kappa$ vertical diffusion of solute is negligible. As before, composition and temperature within the fluid of the mushy layer are coupled by the linear liquidus relationship (4.12). The appropriate interfacial conditions are those of marginal equilibrium (4.21) and conservation of heat across the boundary layer at the moving interface between mush and melt (3.4). Below this interface the melt cools according to (3.3). Finally, to the boundary condition

$$\theta = T_B \quad (z = 0) \tag{5.1}$$

must be added the initial conditions

$$\theta = T_0, \quad C = C_0 \quad (t = 0). \tag{5.2}$$

Solutions to this system of equations were determined numerically. Typical results are presented, with the label of equilibrium growth, in figure 12 which includes data from the experiments using aqueous isopropanol. At first sight the agreement between the theoretical predictions and the experimental data for both the position of the interface and the temperature of the melt appears to be very good (and better than in figure 6!). On closer inspection, however, one notices that the measured temperature of the aqueous isopropanol was always below the predicted temperature, and after approximately 300 min. was also below the liquidus temperature – and by a fairly significant amount (~ 1 °C). That a melt must become locally supersaturated in order for solidification to occur is of course not at all new; what we wish to describe now is the incorporation of the concept of supersaturation into a model that relaxes the assumption that solidification occurs at thermodynamic equilibrium. Aside from leading to better agreement with experimental data, the predictions of the model have far-ranging consequences which include the conditions under which large bodies of melt, such as the molten rock (magma) contained in storage reservoirs within the Earth, can convect when cooled from above (Worster, Huppert & Sparks 1990).

Non-equilibrium processes of crystal growth can be modelled by incorporating the concept that, away from thermodynamic equilibrium, the rate of growth of solid is directly related to the value of the local supersaturation. This concept has a rather broad and old foundation (see, for example, Kurz & Fisher 1986 for a general survey and Flood & Hunt 1987 for an explicit application which has some similarities with that presented here). Our experiments with aqueous isopropanol suggest the simple linear relationship

$$\dot{s} = \mathscr{G}(T_L - T_s) \quad (z = s(t)), \tag{5.3}$$

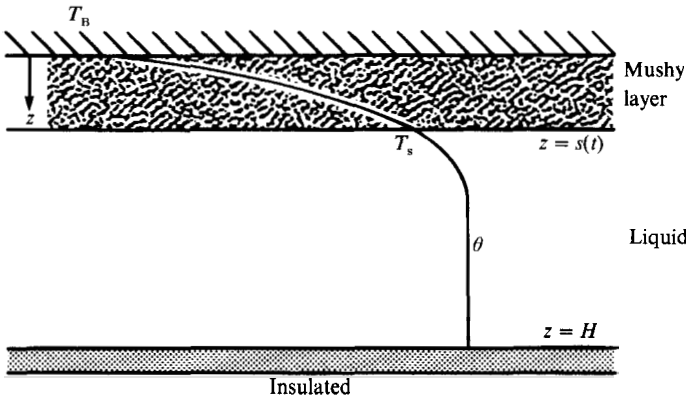

FIGURE 11. Sketch of the temperature profile for a binary melt of initial depth H cooled from above to release melt whose density is less than that of the original melt.

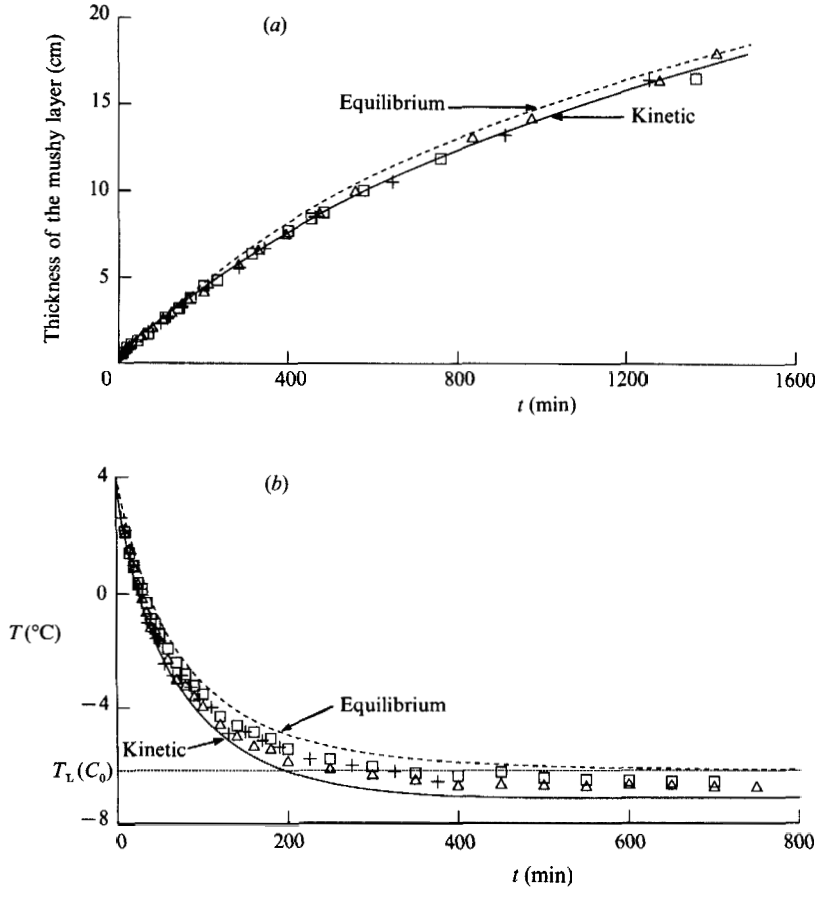

FIGURE 12. (*a*) The thickness of the mushy layer, $s(t)$, and (*b*) the temperature, T, of the aqueous isopropanol as functions of time. The dashed curves are the result of our theoretical model based on the assumption of thermodynamic equilibrium and the solid curves incorporate the kinetic growth law (equation (5.3)). The symbols represent the data from different experiments in which $C_0 = 83.2$ wt% H_2O, $T_0 = 4.0$ °C, $T_B = -17$ °C and $H = 18.8$ cm.

with $T_s < T_L$, where T_L is the liquidus temperature at the interface, T_s is now the *unknown* solidification temperature at the interface and $\mathscr{G}$ is an empirical constant, determined by us for aqueous isopropanol to be 2.2×10^{-4} cm s^{-1} °C^{-1}. More complicated, nonlinear relationships for different substances have been suggested but we found that (5.3) represented a good fit for our data.

The result of incorporating (5.3) into the numerical simulation of our experiments is shown labelled 'kinetic' in figure 12. The theoretical predictions for the position of the solidification front are seen to be in excellent agreement with the experimental data. Those for the temperature of the melt satisfactorily account for the occurrence and time of initiation of the supersaturation but are slightly less than the observed temperatures. We believe that the observed temperatures may have been slightly increased by heat gains from the laboratory.

The fact that in the interior, the melt was at a temperature below its liquidus temperature, and was hence supersaturated, suggests that, were there nucleation sites for crystallization within the melt, there could have been growth additional to that which occurred in the mushy layer. This was not so in our experiments with aqueous isopropanol because the solid ice crystals were lower in density than the original melt and nucleation was not observed in the interior of the solution. On the other hand, our experiments with aqueous sodium sulphate formed relatively heavy sodium sulphate decahydrate crystals, some of which settled to the base of the tank leading to growth of solid at the floor. This illustrates the important concept that under suitable conditions, cooling at the roof of a container leads to crystallization at the floor remote from the site of cooling, as observed previously by THS and described by Brandeis & Jaupart (1986). A description of the theoretical model we developed to account for the growth on the floor is presented in the next section.

6. Compositional stratification in the solid

Stratification of composition in the solid, or zoning as geologists sometimes call it, that results from solidification of a multicomponent melt is important in many different situations. For it to result from a two-component melt, it is necessary that solidification of both component end members occurs. This can result from variation of composition along the solidus, though this is generally a small effect. Indeed for most aqueous solutions it is totally absent. More generally, compositional stratification can only arise if cooling takes place below the eutectic temperature, T_E, the minimum temperature at which the melt can remain liquid, at least at thermodynamic equilibrium.

With the geometry considered in the last section, compositional stratification will result if T_B is maintained below T_E. In this case the thermal profile is as sketched in figure 13 to reflect the experimental evidence shown in figure 14 (plate 1). Commencing from the roof, the first layer, which occupies $0 < z \leqslant s_E(t)$, consists of a composite solid made up of crystals of the two pure end members. The temperature at the boundary $s_E(t)$ is the eutectic temperature T_E. Heat is transferred by conduction through this layer and once the solid is laid down the composition is independent of time. Beneath this solid layer there is a stagnant mushy layer, just as before, which occupies $s_E(t) \leqslant z \leqslant s(t)$. The layer between $z = s(t)$ and $z = s_f(t)$ is occupied by the turbulently convecting melt which transfers heat into the mushy layer. Finally, in $s_f(t) \leqslant z < H$, secondary crystallization leads to a solid layer growing from the floor which we shall take to be of constant composition, say C_f. With time the eutectic front at $z = s_E(t)$ reaches the solid layer growing from the floor and solidification is complete.

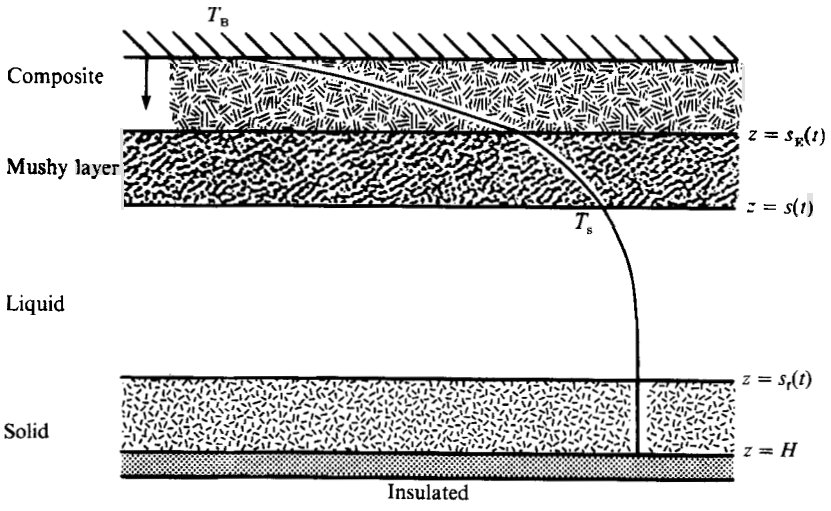

FIGURE 13. Sketch of the temperature profile for a binary melt of initial depth H cooled from above to release melt whose density is less than that of the original melt with the boundary maintained at a temperature that is below the eutectic temperature.

We carried out a series of experiments using aqueous sodium sulphate in order to investigate the situation described above (Kerr *et al.* 1989, 1990*c*). The results of our experimental observations and our theoretical predictions, using the fitted value of $\mathscr{G} = 1.5 \times 10^{-4}$ cm s^{-1} °C^{-1} for aqueous sodium sulphate, are shown for a typical experiment in figure 15. Figure 15(*a*) indicates that the thickness of each of the three layers that are either partially or totally solid grew with time in good agreement with the theoretical predictions. From figure 15(*b*) we see that there is good agreement between our theoretical curves and experimental data for the temperature of the melt as a function of time. For comparison we also draw in the liquidus temperature at the initial concentration. The mean composition in the composite layer decreased with depth from the roof, as is depicted in figure 15(*c*), owing to the gradual decrease in composition of the melt throughout the experiment. There is a discontinuity in mean composition at the height where the downward-growing mushy layer met the upward-growing crystal layer from the floor. The measured compositional profile was fairly well predicted by the theory.

A more complicated situation arises, and new concepts are introduced, on consideration of the cooling from below of a melt that releases less dense fluid on solidification. If the appropriate compositional Rayleigh number is sufficiently large, as we shall assume, compositional effects in this case lead to vigorous mixing of the melt. Aside from the compositional transfers associated with this mixing, there are important thermal transfers to which the compositional transfers are coupled. The coupling arises because the compositional flux determines the intensity of the convective motions in the melt, which in turn determines the thermal flux. This flux regulates the solidification rate and thus the rate at which less dense fluid is released; that is, the compositional flux. Part of the aim of an investigation by Woods & Huppert (1989) was to study the relationship between the compositional flux from, and the thermal flux towards, the interface between melt and solid.

The geometry of our model and the generated profiles of temperature and composition are depicted in figure 16. For simplicity, we neglected all effects due to non-equilibrium thermodynamics and to the formation of a mushy layer at the top

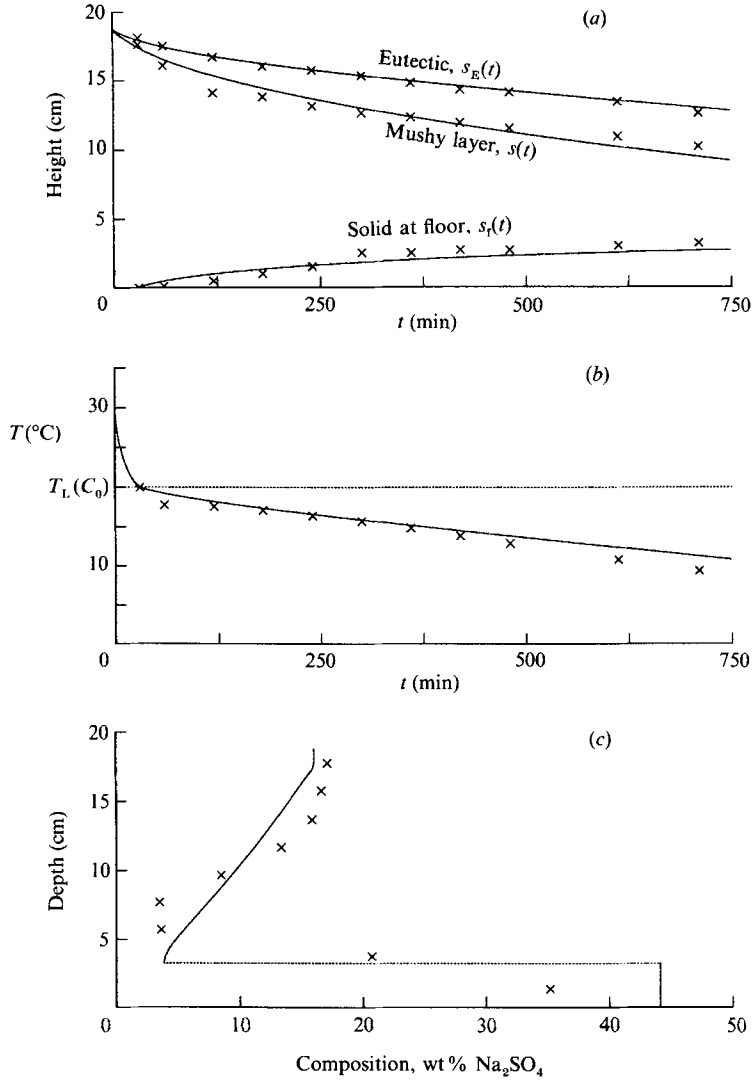

FIGURE 15. The predicted results and experimental data for cooling an aqueous solution of Na_2SO_4 from above for the same values of the physical parameters as in figure 14. (*a*) Height of the three interfaces as functions of time; (*b*) temperature of the liquid as a function of time, and (*c*) composition of the final solid product as a function of depth.

of the crystal pile. Neglecting the latter was an outcome of our experiments with aqueous Na_2CO_3 for which the observed mushy layer was only of order 1 mm thick.

The compositional flux F_C was determined by assuming that the four-thirds law of turbulent thermal convection (cf. (3.3)) can be suitably modified to cover turbulent compositional convection by writing

$$F_C = \gamma_C c(g\beta D^2/\nu)^{\frac{1}{3}}\Delta C^{\frac{4}{3}}, \tag{6.1}$$

where β is the fractional increase in melt density per unit increase in composition, ΔC the compositional change across the compositional boundary layer on top of the solid layer and γ_C an empirical constant which may be different from γ because of the different boundary conditions on heat and composition. Since the turbulent intensity

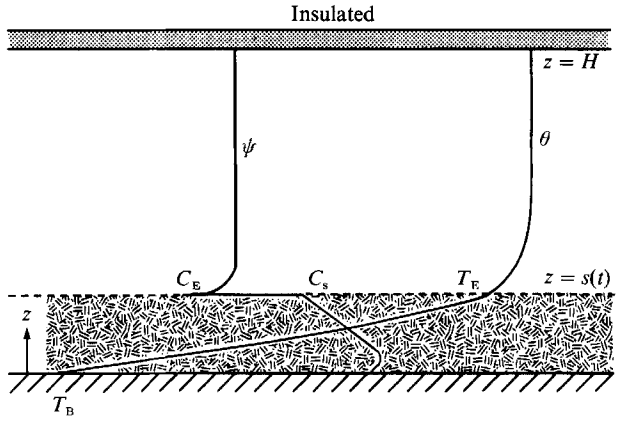

FIGURE 16. Sketch of the temperature and composition profiles for a binary melt of initial depth H cooled from below to release melt whose density is less than that of the original melt with the boundary maintained at below the eutectic temperature.

drives both the thermal and compositional transfers, the non-dimensional heat flux, or thermal Nusselt number, $F_T H/c\kappa\Delta T$, associated with the compositional flux, will be linearly proportional to the compositional Nusselt number $F_C H/cD\Delta C$. The functional relationship, however, may possibly involve the Prandtl number and the ratio of the thermal and compositional diffusivities as well as whether the melt is undersaturated or saturated, since for the latter the temperature and composition in the melt are coupled by the liquidus relationship. Mathematically, this means that

$$F_T = f\left(\frac{\kappa_m}{D}, \frac{\nu}{\kappa_m}\right)\left(\frac{\Delta T}{\Delta C}\right)F_C, \tag{6.2}$$

where f may depend not only on the explicit parameters displayed but also on whether the melt is saturated or undersaturated. When the melt is saturated $\Delta T = m_L \Delta C$ if the liquidus relationship is assumed to be linear. Woods & Huppert (1989) also presented three tentative physical models of the behaviour of the boundary layer at the interface which suggested explicit formulae for f.

The governing equations can then be formulated as follows. Within the solid, the temperature field satisfies the linear equation of heat conduction. However, in order to simplify the analysis, we replaced this with the linear temperature profile

$$T(z,t) = T_B + (T_E - T_B)\,[z/s(t)]. \tag{6.3}$$

This is a good approximation to the full solution of the heat-conduction equation provided that effects due to thermal conduction propagate more rapidly than does the interface between melt and solid. That is, provided $s \ll (\kappa_m t)^{\frac{1}{2}}$. This inequality is generally well satisfied (see, for example, THS and Huppert & Sparks 1988). The incorporation of (6.3) greatly simplifies the analysis because the remaining equations are all ordinary differential equations in time and no partial differential equations need be solved. At the interface between the melt and the solid, conservation of heat requires that (cf. (3.4))

$$k_s(T_E - T_B)/s = fJ_C(\theta - T_E)\,(\psi - C_E)^{\frac{1}{3}} + [c_m(\theta - T_E) + \mathscr{L}]\,\dot{s}, \tag{6.4}$$

where ψ and C_E are the composition of the melt and eutectic respectively and $J_C = \gamma_C(g\beta D^2/\nu)^{\frac{1}{3}}$, while conservation of matter requires that

$$(C_s - \psi)\,\dot{s} = J_c(\psi - C_E)^{\frac{4}{3}}, \tag{6.5}$$

where C_s is the composition of the solid. Within the melt the thermal balance can be written as (cf. (3.3))

$$(H-s)\,\dot{\theta} = -fJ_C(\theta - T_E)\,(\psi - C_E)^{\frac{1}{3}}, \tag{6.6}$$

while conservation of matter requires that

$$(H-s)\,\dot{C}_m = -J_C(\psi - C_E)^{\frac{4}{3}}. \tag{6.7}$$

The system for the four unknowns θ, ψ, C_s and s represented by (6.4)–(6.7) is subject to the initial conditions

$$\theta = T_0, \quad \psi = C_0, \quad C_s = C_0, \quad s = 0 \quad (t = 0), \tag{6.8}$$

where T_0 and C_0 are respectively the initial temperature and concentration of the melt. Equations (6.4)–(6.8), with the one free parameter f, can be integrated numerically (either with or without suitable non-dimensionalization) to lead to theoretical predictions against which laboratory data can be compared.

From experiments with aqueous sodium carbonate, with a fixed value of κ_m/D and ν/κ_m, we found that the data were best fitted by taking $f = 3$ when the melt was undersaturated and $f = 1$ when saturated. The results of a particular integration of (6.4)–(6.8) are graphed in figure 17 and compared with our laboratory data. In figure 17 (a, b), which present comparisons for temperature and composition in the melt and the height of the solid as functions of time, the agreement between theory and experiment are quite good. The agreement in figure 17 (c), which presents the composition of the solid as a function of depth, is not as good, but still quite reasonable. The various segments in the theoretical curve indicate the different fluid regimes under which the solid was formed. For $s < 2.4$ cm ($t < 150$ min) we predicted that the melt would be undersaturated. Beyond these limits saturation was predicted. The various segments of the theoretical curve of figure 17 (c) took up different shapes dependent on the relative balance between the convective and latent heat terms on the right-hand side of (6.4). For most of the segment labelled 1, latent heat was dominant. With time, its relative effect weakened, which lead to the decrease of the composition of the solid with height as convective effects became dominant along the segment marked 2. At the end of this the melt became saturated at which time the model (discontinuously) reduced f from 3 to 1 along the segment marked 3. In reality f will change more gradually and non-equilibrium effects will also occur, which explains the lack of agreement between theory and experiment at this point. The concentration of the solid thereafter adjusted rather rapidly at first to accommodate the discontinuity in the model. Subsequently, along the rest of the segment marked 4, the concentration in the solid slowly decreased as the temperature and concentration of the melt decreased.

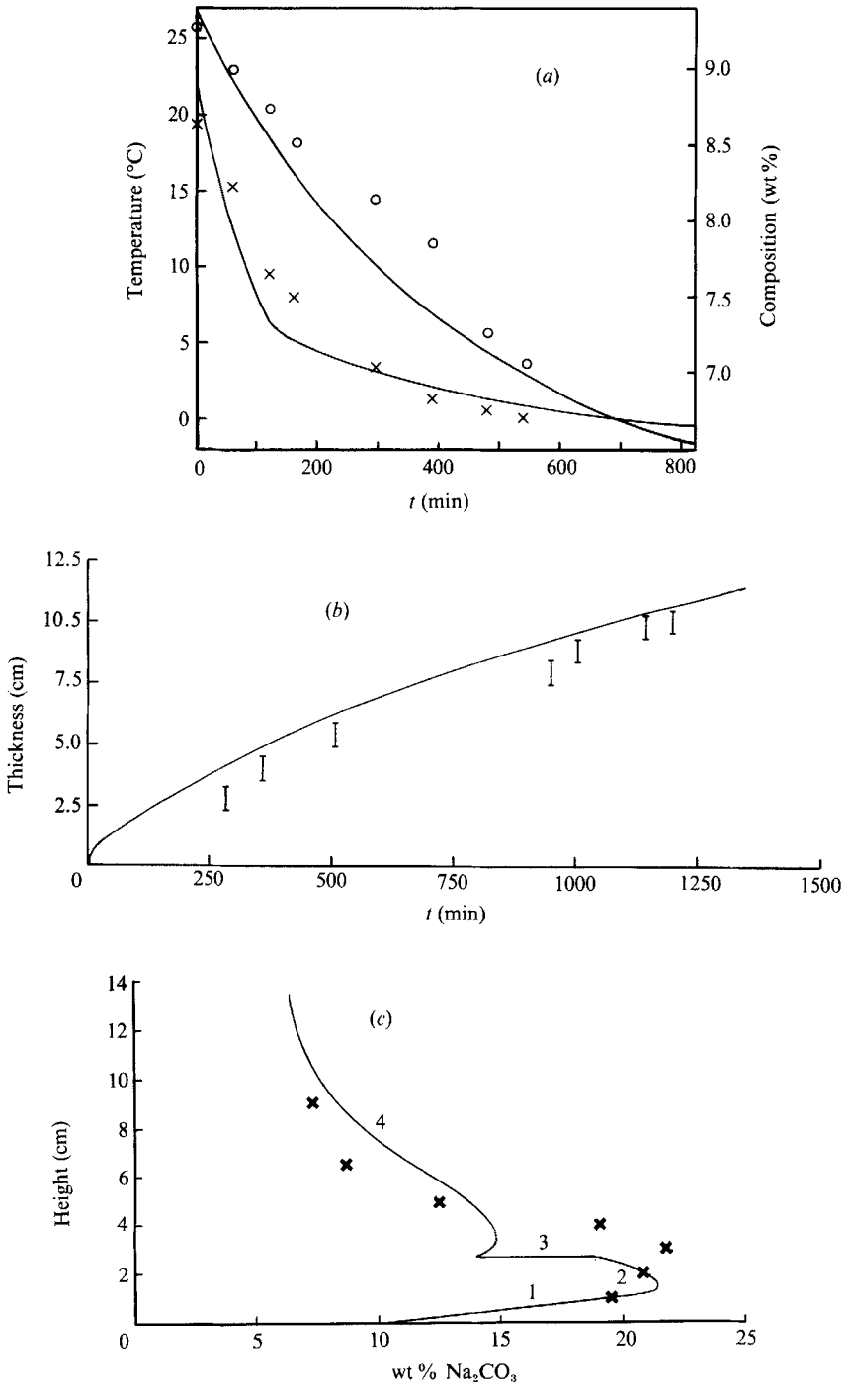

FIGURE 17. The predicted results and experimental data for cooling an aqueous solution of Na_2CO_3 from below with $C_0 = 9.34$ wt% Na_2CO_3, $T_0 = 19.4$ °C, $T_B = -20$ °C and $H = 22$ cm. (*a*) Temperature and composition in the liquid as functions of time; (*b*) thickness of the solid layer as a function of time; and (*c*) composition of the final solid product as a function of depth.

7. The crystallization of aqueous ammonium chloride

To readers new to the subject it will appear strange that a particular aqueous salt is considered in a section by itself. Many laboratory experiments, originating with that described by Copley *et al.* (1970), however, indicate that the formation of NH_4Cl crystals by the cooling of an aqueous ammonium chloride solution from below proceeds in a different way from the solidification of almost all other salts. In particular, as we shall discuss at greater length below, a deep and rather ordered mushy layer results with definite 'chimneys' through which all the less dense, released fluid is channelled. The original impetus by Copley *et al.* (1970) was due to the similarity between these chimneys and 'freckles' – long finger-like regions of compositional segregation – which are often observed in castings of steel and binary alloy systems such as aluminum–copper, lead–tin and nickel–aluminum. These freckles represent undesirable imperfections in the casting. Both because of the metallurgical importance and because of the pure scientific interest, it could be said that one of the 'prizes' of the subject is a thorough understanding of the phenomena observed in aqueous NH_4Cl. Furthermore, there are possible applications to the formation of the solid inner core of the Earth.

The laboratory experiment is easy to perform and makes a simple and attractive fluid-dynamical demonstration. An aqueous ammonium chloride solution of composition more concentrated than the eutectic value (20 wt %)† is placed in a suitable container (a glass beaker will do) and cooled from below – by placing the beaker in a cold brine solution, for example. After a short while a partially solid layer of pure NH_4Cl crystals forms and the thickness of the layer gradually increases. The NH_4Cl solution above the crystals remains continually undersaturated, as is indicated in figure 18(*a*). This is in marked and important contrast to the supersaturated solution which quickly develops above the solid formed on the cooling of any other aqueous solution whose concentration is beyond the eutectic value, as indicated for the particular example of Na_2CO_3 in figure 18(*b*). In the case of NH_4Cl the circulation consists of isolated buoyant plumes (see figure 19*a*, plate 2) which drive a return flow of the undersaturated solution. This slowly migrates towards the layer of crystals and flows down into it. Because the flow through the crystals takes place in a decreasing temperature field, the aqueous solution becomes saturated and builds up further pure NH_4Cl crystals, which exhibit beautiful secondary and tertiary branching, as depicted in figure 19(*b*) (plate 2). The NH_4Cl-depleted solution from a wide area flows to a central point and the less dense return flow takes place through a few isolated chimneys, as indicated in figure 19(*a*, *c*) (plates 2, 3). With time some chimneys 'die' and the overall intensity of the convective motion decreases as the thickness of the mushy layer increases. This flow pattern is quite different from that produced by all other aqueous solutions, as shown for the typical example of Na_2CO_3 in figure 20 (plate 3).

In my opinion, no satisfactory quantitative model of the flow, evolution of the chimneys and growth of the crystals has yet been proposed, although interesting attempts at the full problem have been presented by Roberts & Loper (1983) and Fowler (1985). There is not even agreement as to why the phenomena described occur only for NH_4Cl solutions. Indeed, I have heard it said that chimneys can be seen under suitable conditions for all solutions, though in a variety of experiments with

† At 20 °C the liquidus is at 28 wt % and the solution needs to be initially warmed from room temperature if a solution of greater concentration is desired.

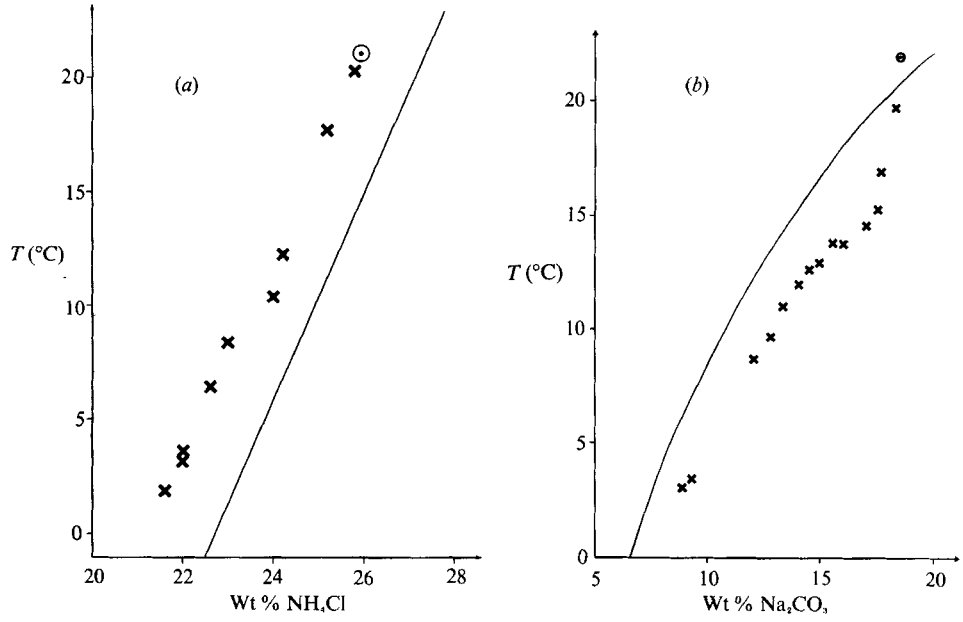

FIGURE 18. Temperature in the liquid as a function of its concentration for (*a*) NH_4Cl and (*b*) Na_2CO_3. The curves are the liquidii and the crosses are experimental data. The experiments started at ⊙.

numerous salts I have never observed chimneys other than for aqueous NH_4Cl. Included among the suggested explanations of why NH_4Cl is special are: the crystal mush is of low solid fraction; the energy of formation is high; the crystal has no water of hydration (though this is true of other crystals); the liquidus curve is particularly steep; the concentration of NH_4Cl at the solidus is so much larger than that in the original solution; and that NH_4Cl crystals are much less faceted than those of all other salts.

8. Cooling at a sidewall

Cooling and crystallizing a melt from the side requires another spatial dimension to be considered because horizontal thermal and compositional gradients interact with the predominantly vertical flow of released fluid due to the vertical orientation of gravity. The situation of pure cooling (or heating) without crystallization at a semi-infinite wall is by now a classical problem in fluid mechanics (see, for example, Ostrach 1964 or Chapman 1984). The inclusion of crystallization adds two new effects – one due to the presence of compositional influences in addition to thermal influences and the other due to the moving boundary between solid and melt. The incorporation of both these effects together has resisted analytical investigation. On the assumption that the effects of crystallization can be treated by specifying a thermal and compositional anomaly at the (fixed) wall, and hence neglecting the solid regime that is formed, a number of authors have presented boundary-layer analyses of flow past a vertical wall in an infinite fluid (Nilson & Baer 1982; Spera, Yuen & Kemp 1984; Nilson 1985; Nilson, McBirney & Baker 1985).

All these studies have focused on the situation for which the density anomaly at the wall due to temperature, $\Delta\rho_T$, is positive, which corresponds to a cooled wall and by itself would induce downwards motion, while the density anomaly at the wall due

to composition, $\Delta\rho_C$, is negative, which corresponds to the release of less dense fluid and by itself induces upwards motion. This situation has received maximum attention because it is the one most relevant to a geological context. It is also the one that arouses most fluid-mechanical interest because of the inherent possibility of a bi-directional boundary layer. In the limit $D \ll \kappa \ll \nu$ three separate boundary-layer regions can be discerned. In the inner region, which is closest to the wall, compositional buoyancy forces due to compositional differences balance viscous forces. Beyond this, in an intermediate region, buoyancy forces due to thermal differences balance viscous forces. Finally, in the furthest region, the inner and intermediate motions are responded to by viscous coupling with the inertia forces. The flow and relative strengths of the boundary layers depend on only three external parameters: the Prandtl number $Pr = \nu/\kappa$; the ratio of the diffusivities $\tau = D/\kappa$; and the (positive) ratio $r = -\Delta\rho_T/\Delta\rho_C$. For sufficiently small r compositional effects overpower thermal effects and the entire flow is predicted to be upwards. For sufficiently large r thermal effects dominate and the entire flow is downwards. For intermediate values of r a bi-directional motion results, with an upwards inner flow and a downwards intermediate flow. For large Pr, Nilson (1985) showed that the bi-directional flow occurred whenever $0.62\tau < r < 1.09\tau^{\frac{1}{3}}$. On the further assumption that $\tau \ll 1$, as is typically the case, Nilson used asymptotic expansions to match the inner upward-flowing boundary layer, whose width increased as $x^{\frac{1}{4}}$, where x is distance from the base of the wall, to the very much thicker downward-flowing boundary layer whose width increased as $(L-x)^{\frac{1}{4}}$, where L is the total length of the wall. A typical example of the resulting self-similar vertical velocity, adapted from Nilson *et al.* (1985), is drawn in figure 21.

A similar calculation assuming that the flow takes place in a porous medium has been conducted by Lowell (1985) who also suggests that the value of r determines whether the flow is all upwards or all downwards or takes place in a bi-directional boundary layer. Such bi-directional boundary-layer flows are fairly easy to set up and visualize in a laboratory experiment.

These analytical calculations have all assumed that the ambient conditions far from the wall are constant. If the wall is part of a container, the boundary-layer flows alter the environment and in turn are altered by it. This brings about new phenomena. Some of these have been investigated from an experimental point of view (see, for example, McBirney 1980; Turner 1980; Turner & Gustafson 1981; McBirney, Baker & Nilson 1985 and Leitch 1987), while the work of Thompson & Szekely (1987, 1988) is, to my knowledge, the only theoretical study yet published. The latter authors also conducted laboratory experiments with which to compare their numerical calculations.

The major conclusion of all these studies is that solidification from the side of an initially homogeneous solution results in the formation of a vertical composition gradient in the melt. The gradient results from the convection driven by the fluid released on solidification, whether it be more or less dense than the original fluid. Cooling a vertical compositional gradient from the side leads to an array of nearly horizontal double-diffusive layers separated by sharp interfaces (see, for example, Huppert & Turner 1980 and references therein). A photograph of a typical experiment, showing the layering and somewhat irregular interface between fluid and solid, appears as figure 22 (plate 4). Figure 23, kindly given to me by Mollie Thompson, is the result of her numerical calculations of a similar situation, though the explicit values of the physical parameters are different. The initial development of double-diffusive layers in the calculations is clearly evident, but more computer time would

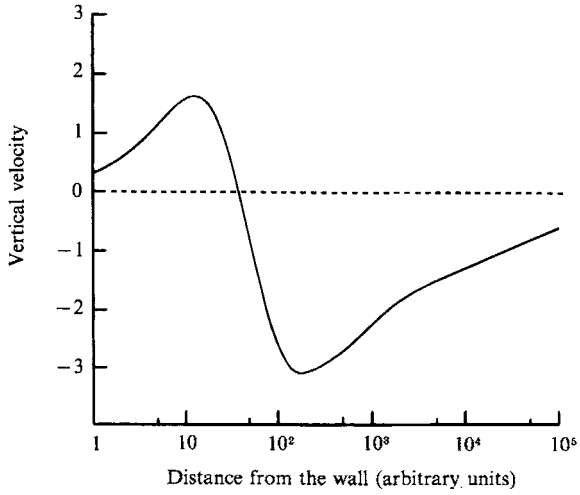

FIGURE 21. The self-similar vertical velocity as a function of distance from a wall which is maintained at a decreased temperature and an increased composition over the far-field value.

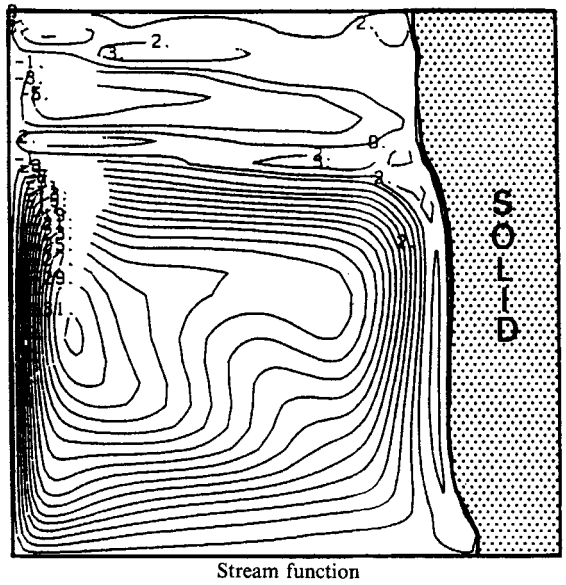

FIGURE 23. The result of numerical calculations performed by M. E. Thompson on cooling an aqueous solution of Na_2CO_3 at a sidewall.

be needed to simulate the further evolution. My student, Richard Jarvis, is currently developing a more general and powerful numerical program, which we hope will provide useful and interesting results in the future.

Aside from the stratification set up in the fluid, there is also compositional stratification in the resulting solid product. In her dissertation, Leitch (1985) extended the earlier pioneering work of Turner & Gustafson (1981) to discuss experiments in which initially uniform solutions of aqueous sodium carbonate were cooled from a sidewall of a tank $16 \times 20 \times 15$ cm high. The refrigeration unit that provided the coolant was operated at its maximum power; thus the temperature of

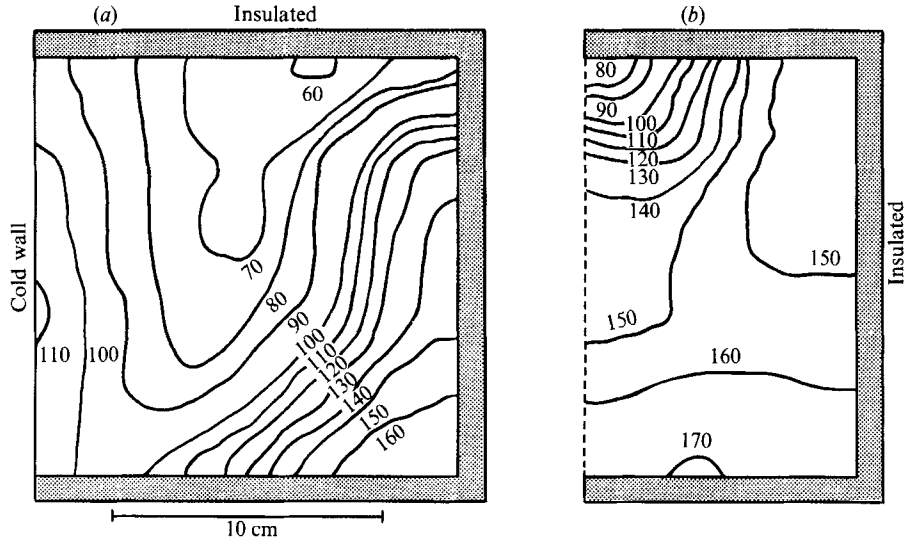

FIGURE 24. The distribution of composition, in units of kg of $Na_2CO_3.10\ H_2O$ per m^3 of solution, in the solid product obtained by cooling an initially homogeneous aqueous solution of Na_2CO_3 at a vertical wall. The initial composition was 111 kg of $Na_2CO_3.10\ H_2O$ per m^3 of solution. (*a*) The concentration in the middle plane of the tank, parallel to two insulated sides; (*b*) the concentration in half the transverse section at the insulated end of (*a*).

the cold wall was not controlled (though it was recorded). The resulting distribution of composition in the solid, measured at the end of the experiment for which the initial concentration of Na_2CO_3 was less than the eutectic value, is shown in figure 24. Considerable spatial variations in composition, both in the horizontal and in the vertical, are clearly evident, though these variations are not yet quantitatively understood. Similar variations in the resulting solid composition were reported by Hebditch (1975), who solidified melts composed of lead and tin by cooling them at a vertical wall. The broad similarity between the results of these two sets of experiments indicate that the phenomena seen in aqueous salt solutions are replicated in other fluids with widely different properties.

9. Crystallization on a slope

Many of the principles enunciated in the previous sections are displayed in the study of crystallization resulting from cooling at a slope. In a series of experiments reported in Huppert *et al.* (1986, 1987) we inserted a cooling plate at an angle to the vertical into the interior of an aqueous solution. A particularly illustrative case is that in which the slope is at 45° to the vertical and is inserted symmetrically into the container. The slope then divides the fluid into two geometrically identical regions. If convective effects were absent, solidification would proceed identically in the two regions. However, as can be seen in figure 25 (plate 4), the influence of convection is dominant though different in the two regions.

In some of the experiments we used an initially homogeneous solution of sodium carbonate whose concentration was greater than the eutectic value. In both regions less dense fluid was released by the crystallization on the upper and lower surfaces of the cooling plate. Above the plate the released fluid was free to rise and did so in a series of plumes which mixed with the environment to produce a complicated large-

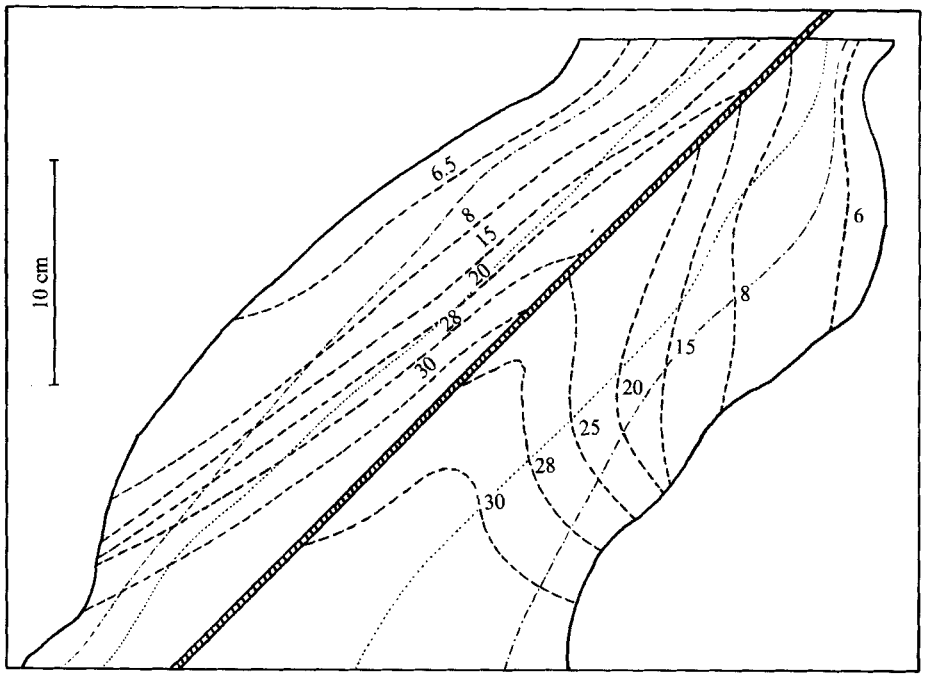

FIGURE 26. The distribution of composition, reproduced from Huppert *et al.* (1987), in units of wt % Na_2CO_3, in the solid product obtained by cooling an initially stratified aqueous solution of Na_2CO_3 at a 45° slope. The initial composition increased linearly from 6 wt % at the top of the tank to 13 wt % at the bottom. The solidification front after 55 hours is indicated by · · · · and after 73 hours by -·-·-.

scale flow. Part of the flow consisted of strong motions up the slope of fluid from the interior entrained into the boundary layer and drawn towards the sites of crystallization. Another part of the flow was driven by the horizontal density gradients set up by the different heights of the plumes and hence different amounts of mixing along the slope. The released fluid which formed below the plate, on the other hand, was not free to rise because of the constraint of the overlying plate. The fluid slowly migrated through the crystal mush and was deposited at the top of the layer. Because of the cooling, the temperature of the interior decreased with time and so the density of the released fluid decreased also, in accord with the phase diagram of figure 1. Thus newly released fluid flowed to the top of the region and displaced downwards the fluid previously deposited there, just as in the now classical 'filling-box' situation (Baines & Turner 1969; Worster & Leitch 1985 and Baines, Turner & Campbell 1990). As in that situation, the sharp interface between the released fluid and the initial fluid propagated downwards and a quite strongly stratified, virtually stagnant fluid region evolved above the interface. As seen in figure 25, the macroscopic crystal structure took three forms: above the slope there was a very smooth interface between the crystals and the fluid due to the strong up-slope motions in the latter; in the lower part of the downward-facing surface, the interface was fairly convoluted owing to the fluid being irregularly crystallized at randomly oriented nucleation sites, while in the upper part of the surface there were much longer crystals and a more convoluted interface. With time, the interface in the left-hand region reached the bottom and eventually all the remaining fluid to the left of

the slope was at the eutectic composition. In the right-hand region, horizontal thermal and compositional gradients induced the ubiquitous double-diffusive layering and strong velocity gradients. (These are just beginning to form at the time the photograph in figure 25 was taken.)

Experiments which commenced with a vertical gradient of composition (Huppert *et al.* 1987) showed again that vertical density gradients have a strong restraining influence on compositional convection. A series of double-diffusive layers evolved, with thin plumes only occasionally penetrating one of the interfaces. Owing to the large molecular diffusivity of heat in comparison with that of composition, the circulation in the double-diffusive layers was controlled by thermal effects, even in regions where the plume motion due to compositional convection partially opposed the sense of motion. The compositional variations in the solid resulting from one experiment are shown in figure 26.

There are clearly a number of fluid-dynamical aspects of this situation that need quantitative investigation. It would be fruitful to construct a numerical program that incorporates the strong convective flows in the melt, the dynamics of the mushy zone behind the crystallization front and the possibility of compositional stratification in the solid product. Such an advance represents a challenging task for the future.

10. Applications

Although there are obviously many different industrial and natural applications of the concepts outlined in the previous sections, to discuss them at length here would unbalance the overall presentation. There appear to be four main broad areas of application: metallurgy, geology, geophysics and crystal growth. We expand on each of these in one or two paragraphs below.

The formation of solid castings from liquid melts is a central area of metallurgy. A knowledge of the time taken for solidification to be completed can have large financial consequences. In addition, the strength of the final product may depend critically on the existence of any macroscopic inhomogeneities. These can result from convection within the mould, which as well as influencing the macroscopic form of the final product (cf. figure 25) can also determine the final deposition site of any small impurities in the original melt that do not easily solidify, or may even be totally incompatible.

My own interest in solidification problems originally arose from a geological context. Approximately 20 km^3 of molten rock or magma are produced within the Earth each year and this melt solidifies in magma chambers, along lava flows and during volcanic eruptions. Geologists use the data they collect from the resulting solid rock suites as a means of understanding the processes that take place within the Earth. Fluid mechanics clearly is an essential ingredient, although it was rather neglected by geologists until recently (see, for example, Huppert 1986 for an elaboration of this argument). The idea that the compositional zonation which is observed in rock suites could have been formed in the original fluid state (cf. figure 22) rather than in the solid state was initially put forward by Chen & Turner (1980) in a paper which can be considered as the commencement of a systematic attempt to introduce fluid-mechanical concepts into geology. This has led to an understanding of the formation of numerous rock suites around the world, some of which have associated ore deposits (see THS).

The core problem in geophysics that is probably determined by solidification is an

explanation of how the magnetic field of the Earth is maintained. A popular view at the moment, first proposed by Braginskii (1963), is that the solidification of the solid inner core releases less dense fluid which rises through the liquid outer core. In doing so, Coriolis forces, due to the rotation of the Earth, and Lorentz forces, due to the motion of a conducting medium through an existing magnetic field, combine to maintain the geodynamo. There is still much to be quantitatively understood before this view can be demonstrated to be correct.

More needs to be known about the formation of both the solid inner core and the mushy layer which may well be associated with it. A series of papers has attempted to develop a general thermodynamic approach of the formation of mushy layers and slurries and then apply the results to an investigation of the processes that occur at the inner core boundary (see, for example, Loper & Roberts 1978, 1980; Loper 1983 and Hills, Loper & Roberts 1983). However, in my view at least, because the theory is so general and the number of explicit solutions derived from it so few, with no real experimental tests yet considered, it is not currently possible to know how applicable most of the approximations built into the model are. Another question, which is virtually unexplored, is how the rising buoyant plumes are influenced by rotation, though an investigation in terms of fluid parcels has been commenced by Moffatt (1989).

To crystal growers, obtaining a uniform final solid product is one, if not the most, essential aspect of their craft. Instabilities, convection, mushy zones, and compositional stratification are all anathema to them. By understanding under what conditions such fluid-mechanical effects can occur, the crystal grower has taken the first step in understanding how to eliminate them.

11. Conclusions

We conclude that fluid-mechanical effects can play a dominant role in many solidification problems. This paper has concentrated on reviewing one approach to the subject, namely a systematic development of the concepts involved when a liquid is uniformly cooled at a flat surface. Further investigations using this approach could be interestingly contemplated. The investigations could include the determination of a full quantitative understanding of both the effects due to cooling at a sloping surface and the influence of initial compositional stratification in the liquid. In addition, different approaches to problems in phase transitions, some briefly described and referenced in this review, can be fruitfully extended. In short, there is still much of interest to be uncovered regarding the fluid mechanics of solidification considered from any of the points of view traditionally taken up by applied mathematicians, crystal growers, engineers, geologists, geophysicists or physicists.

It is a pleasure to dedicate this review to my colleague and mentor, George Batchelor. His leadership, inspiration and encouragement of research over a broad range of fluid mechanics has helped make my 21 years in Cambridge extremely exciting and rewarding. Helpful reviews of earlier drafts were given to me by S. H. Davis, D. T. J. Hurle, R. A. Jarvis, R. C. Kerr, A. R. McBirney, J. S. Turner, A. W. Woods and M. G. Worster, to all of whom I am grateful. Mark Hallworth has unstintingly helped with all my experiments described here and produced almost all the figures. My research is supported by the British Petroleum Venture Research Unit.

REFERENCES

ANANTH, R. & GILL, W. N. 1988 The effect of convection on axisymmetric parabolic dendrites. *Chem. Engng. Commun.* **68**, 1–14.

ANANTH, R. & GILL, W. N. 1989 Dendritic growth of an elliptical paraboloid with forced convection in the melt. *J. Fluid Mech.* **208**, 575–593.

BAINES, W. D. & TURNER, J. S. 1969 Turbulent buoyant convection from a source in a confined region. *J. Fluid Mech.* **37**, 51–80.

BAINES, W. D., TURNER, J. S. & CAMPBELL, I. H. 1990 Turbulent fountains in an open chamber. *J. Fluid Mech.* **212**, 557–592.

BATCHELOR, G. K. 1974 Transport properties of two-phase materials with random structure. *Ann. Rev. Fluid Mech.* **6**, 227–255.

BRAGINSKII, S. I. 1963 Structure of the F layer and reasons for convection in the Earth's core. *Sov. Phys. Dokl.* **149**, 8–10.

BRANDEIS, G. & JAUPART, C. 1986 On the interaction between convection and crystallization in cooling magma chambers. *Earth Planet. Sci. Lett.* **77**, 345–361.

BROWN, R. A. 1988 Theory of transport processes in single crystal growth from the melt. *AIChEJ.* **34**, 881–911.

CANRIGHT, D. & DAVIS, S. H. 1989 Similarity solutions for phase-change problems. *Metall. Trans.* A **20**, 225–235.

CARSLAW, H. S. & JAEGER, J. C. 1959 *Conduction of Heat in Solids*. Cambridge University Press.

CHAPMAN, A. J. 1984 *Heat Transfer*. Macmillan.

CHEN, C.-F. & TURNER, J. S. 1980 Crystallization in a double-diffusive system. *J. Geophys. Res.* **85**, 2573–2593.

COPLEY, S. M., GIAMEI, A. F., JOHNSON, S. M. & HORNBECKER, M. F. 1970 The origin of freckles in unidirectionally solidified castings. *Metall. Trans.* **1**, 2193–2204.

CORIELL, S. R., CORDES, M. R., BOETTINGER, W. J. & SEKERKA, R. F. 1980 Convective and interfacial instabilities during unidirectional solidification of a binary alloy. *J. Cryst. Growth* **49**, 13–28.

CORIELL, S. R., MCFADDEN, G. B. & SEKERKA, R. F. 1985 Cellular growth during directional solidification. *Ann. Rev. Mater. Sci.* **15**, 119–145.

CRANK, J. 1984 *Free- and Moving-Boundary Problems*. Clarendon.

DAVIS, S. H. 1990 Hydrodynamic interactions in directional solidification. *J. Fluid Mech.* **212**, 241–262.

DAVIS, S. H., MÜLLER, U. & DIETSCHE, C. 1984 Pattern selection in single-component systems coupling Bénard convection and solidification. *J. Fluid Mech.* **144**, 133–157.

DIETSCHE, C. & MÜLLER, U. 1985 Influence of Bénard convection on solid–liquid interfaces. *J. Fluid Mech.* **161**, 249–268.

FLOOD, S. & HUNT, J. D. 1987 A model of a casting. *Appl. Sci. Res.* **44**, 27–42.

FOWLER, A. C. 1985 The formation of freckles in binary alloys. *IMA J. Appl. Maths* **35**, 159–174.

GLEICK, J. 1988 *Chaos*. Heinemann.

GLICKSMAN, M. E., CORIELL, S. R. & MCFADDEN, G. B. 1986 Interaction of flows with the crystal–melt interface. *Ann. Rev. Fluid Mech.* **18**, 307–335.

HEBDITCH, D. J. 1975 Contribution concerning the solidification problem. In *Moving Boundary Problems in Heat Flow and Diffusion* (ed. J. R. Ockendon & W. R. Hodgkins). Clarendon.

HILL, J. M. 1987 *One-dimensional Stefan Problems: An Introduction*. Longman.

HILLS, R. N., LOPER, D. E. & ROBERTS, P. H. 1983 A thermodynamically consistent model of a mushy zone. *Q.J. Appl. Maths* **36**, 505–539.

HUPPERT, H. E. 1986 The intrusion of fluid mechanics into geology. *J. Fluid Mech.* **173**, 557–594.

HUPPERT, H. E. & SPARKS, R. S. J. 1988 Melting the roof of a chamber containing a hot, turbulently convecting fluid. *J. Fluid Mech.* **188**, 107–131.

HUPPERT, H. E., SPARKS, R. S. J., WILSON, J. R. & HALLWORTH, M. A. 1986 Cooling and crystallization at an inclined plane. *Earth Planet. Sci. Lett.* **79**, 319–328.

HUPPERT, H. E., SPARKS, R. S. J., WILSON, J. R., HALLWORTH, M. A. & LEITCH, A. M. 1987 Laboratory experiments with aqueous solutions modelling magma chamber processes. II. Cooling and crystallization along inclined planes. In *Origins of Igneous Layering*, pp. 539–568. NATO Advanced Studies Institute. Reidel.

HUPPERT, H. E. & TURNER, J. S. 1980 Ice blocks melting into a salinity gradient. *J. Fluid Mech.* **100**, 367–384.

HUPPERT, H. E. & WORSTER, M. G. 1985 Dynamic solidification of a binary melt. *Nature* **314**, 703–707.

HURLE, D. T. J., JAKEMAN, E. & WHEELER, A. A. 1982 Effect of solutal convection on the morphological stability of a binary alloy. *J. Cryst. Growth* **58**, 163–179.

IVANTSOV, G. P. 1947 Temperature field around spherical, cylindrical and needle-shaped crystals growing in a supercooled melt. *Dokl. Akad. Nauk SSSR* **58**, 567–569.

KERR, R. C., WOODS, A. W., WORSTER, M. G. & HUPPERT, H. E. 1989 Disequilibrium and macrosegregation during solidification of a binary melt. *Nature* **340**, 357–362.

KERR, R. C., WOODS, A. W., WORSTER, M. G. & HUPPERT, H. E. 1990*a* Solidification of an alloy cooled from above. Part 1. Equilibrium growth. *J. Fluid Mech.* (in press).

KERR, R. C., WOODS, A. W., WORSTER, M. G. & HUPPERT, H. E. 1990*b* Solidification of an alloy cooled from above. Part 2. Non-equilibrium interfacial kinetics. *J. Fluid Mech.* (in press).

KERR, R. C., WOODS, A. W., WORSTER, M. G. & HUPPERT, H. E. 1990*c* Solidification of an alloy cooled from above. Part 3. Compositional stratification within the solid. *J. Fluid Mech.* (in press).

KURZ, W. & FISHER, D. J. 1986 *Fundamentals of Solidification*. Trans. Tech. Publications.

LAMÉ, G. & CLAPEYRON, B. P. 1831 Mémoire sur la solidification par refroidissement d'un globe solide. *Ann. Chem. Phys.* **47**, 250–256.

LANGER, J. S. 1980 Instabilities and pattern formation in crystal growth. *Rev. Mod. Phys.* **52**, 1–28.

LANGER, J. S. 1987 Lectures in the theory of pattern formation. In *Chance and Matter*, pp. 629–712. Les Houches session XLVI Nato ASI. North-Holland.

LEITCH, A. M. 1985 Laboratory models of magma chambers. Ph.D. thesis, Australian National University.

LEITCH, A. M. 1987 Various aqueous solutions crystallizing from the side. In *Structure and Dynamics of Partially Solidified Systems* (ed. D. E. Loper), pp. 37–57. Martinus Nijhoff.

LOPER, D. E. 1983 Structure of the inner core boundary. *Geophys. Astrophys. Fluid Dyn.* **25**, 139–155.

LOPER, D. E. 1987 *Structure and Dynamics of Partially Solidified Systems*. Martinus Nijhoff.

LOPER, D. E. & ROBERTS, P. H. 1978 On the motion of an iron-alloy core containing a slurry. I. General theory. *Geophys. Astrophys. Fluid Dyn.* **9**, 289–321.

LOPER, D. E. & ROBERTS, P. H. 1980 On the motion of an iron-alloy core containing a slurry. II. A simple model. *Geophys. Astrophys. Fluid Dyn.* **16**, 83–127.

LOWELL, R. P. 1985 Double-diffusive convection in partially molten silicate systems: its role during magma production and in magma chambers. *J. Volcanol. Geotherm. Res.* **26**, 1–24.

MCBIRNEY, A. R. 1980 Mixing and unmixing of magmas. *J. Volcanol. Geotherm. Res.* **7**. 357–371.

MCBIRNEY, A. R., BAKER, B. H. & NILSON, R. H. 1985 Liquid fractionation. Part I: basic principles and experimental simulations. *J. Volcanol. Geotherm. Res.* **24**, 1–24.

MOFFATT, H. K. 1989 Liquid metal MHD and the geodynamo. In *Proc. IUTAM Symposium on Liquid Metal Magnetohydrodynamics, Riga, USSR, May 1988*. Kluwer Academic Publications.

MULLINS, W. W. & SEKERKA, R. F. 1964 Stability of a planar interface during solidification of a dilute binary alloy. *J. Appl. Phys.* **35**, 444–451.

NILSON, R. H. 1985 Countercurrent convection in a double-diffusive boundary layer. *J. Fluid Mech.* **160**, 181–210.

NILSON, R. H. & BAER, M. R. 1982 Double-diffusive counterbuoyant boundary layer in laminar natural convection. *Intl J. Heat Mass Transfer* **25**, 285–287.

NILSON, R. H., MCBIRNEY, A. R. & BAKER, B. H. 1985 Liquid fractionation. Part II: fluid dynamics and quantitative implictions for magmatic systems. *J. Volcanol. Geotherm. Res.* **24**, 25–54.

OSTRACH, S. 1964 Laminar flows with body forces. In *Theory of Laminar Flows* (ed. F. K. Moore). Princeton University Press.

ROBERTS, P. H. & LOPER, D. E. 1983 Towards a theory of the structure and evolution of a dendrite layer. In *Stellar and Planetary Magnetism* (ed. A. M. Soward), pp. 329–349. Gordon and Breach.

RUBINSTEIN, L. 1971 *The Stefan Problem.* AMS Transl. vol. 27, American Mathematical Society, Providence, RI.

RUTTER, J. W. & CHALMERS, B. 1953 Prismatic substructure. *Can. J. Phys.* **31**, 15–39.

SPERA, F. J., YUEN, D. A. & KEMP, D. V. 1984 Mass transfer rates along vertical walls in magma chambers and magma upwelling. *Nature* **310**, 764–767.

STEFAN, J. 1889 Über einige Probleme der Theorie der Wämeleitung. *S.-B. Wien. Akad. Mat. Natur.* **98**, 473–484.

THOMPSON, M. E. & SZEKELY, J. 1987 Double-diffusive convection during solidification at a vertical wall. In *Structure and Dynamics of Partially Solidified Systems.* (ed. D. E. Loper). Martinus Nijhoff.

THOMPSON, M. E. & SZEKELY, J. 1988 Mathematical and physical modelling of double-diffusive convection of aqueous solutions crystallizing at a vertical wall. *J. Fluid Mech.* **187**, 409–433.

TURNER, J. S. 1979 *Buoyancy Effects in Fluids.* Cambridge University Press.

TURNER, J. S. 1980 A fluid-dynamical model of differentiation and layering in magma chambers. *Nature* **255**, 213–215.

TURNER, J. S. & GUSTAFSON, L. B. 1981 Fluid motions and compositional gradients produced by crystallization or melting at vertical boundaries. *J. Volcanol. Geotherm. Res.* **11**, 93–125.

TURNER, J. S., HUPPERT, H. E. & SPARKS, R. S. J. 1986 Komatiites II: Experimental and theoretical investigations of post-emplacement cooling and crystallization. *J. Petrol.* **27**, 397–437 (herein THS).

WOODS, A. W. & HUPPERT, H. E. 1989 The growth of compositionally stratified solid above a horizontal boundary. *J. Fluid Mech.* **199**, 29–53.

WORSTER, M. G. 1983 Convective flow problems in geological fluid dynamics. Ph.D. thesis, University of Cambridge.

WORSTER, M. G. 1986 Solidification of an alloy from a cooled boundary. *J. Fluid Mech.* **167**, 481–501.

WORSTER, M. G., HUPPERT, H. E. & SPARKS, R. S. J. 1990 Convection and crystallization in magma cooled from above. *Earth Planet. Sci. Lett.* (submitted).

WORSTER, M. G. & LEITCH, A. M. 1985 Laminar free convection in confined regions. *J. Fluid Mech.* **156**, 301–319.